Harvest-and-Opportunistically-Relay: Analyses on Transmission Outage and Covertness

Yuanjian Li, Rui Zhao, *Member, IEEE*, Yansha Deng, *Member, IEEE*, Feng Shu, *Member, IEEE*, Zhiqiao Nie, and A. Hamid Aghvami, *Life Fellow, IEEE*

***Abstract*— To enhance transmission performance, privacy level, and energy manipulating efficiency of wireless networks, this article initiates a novel simultaneous wireless information and power transfer (SWIPT) full-duplex (FD) relaying protocol, named harvest-and-opportunistically-relay (HOR). Due to the FD characteristics, the dynamic fluctuation of relay's residual energy is difficult to quantify and track. To solve this problem, the Markov Chain (MC) theory is invoked. Furthermore, to improve the privacy level of the proposed HOR relaying system, covert transmission performance analysis is performed, where closed-form expressions of the optimal detection threshold and minimum detection error probability are derived. Last but not least, with the aid of stationary distribution of the MC, closed-form expression of transmission outage probability is calculated, based on which transmission outage performance is analyzed. Numerical results have validated the correctness of analyses on transmission outage and covertness. The impacts of key system parameters on the performance of transmission outage and covertness are given and discussed. Based on mathematical analysis and numerical results, we showcase that the proposed HOR model can not only reliably enhance the transmission performance via smartly managing residual energy but also efficiently improve the privacy level of the legitimate transmission party via dynamically adjusting the optimal detection threshold.**

***Index Terms*— Markov chain, energy harvesting, full-duplex, covert communications, performance analysis.**

Manuscript received February 25, 2020; revised June 9, 2020; accepted August 2, 2020. Date of publication August 19, 2020; date of current version December 10, 2020. This work was supported in part by the Natural Science Foundation of Fujian Province under Grant 2019J01055 and in part by the Promotion Program for Young and Middle-Aged Teacher in Science and Technology Research of Huaqiao University under Grant ZQN-PY407. The work of Yuanjian Li was supported by the China Scholarship Council and King's College London for their Joint Full-Scholarship (K-CSC) to pursue his full-time Ph.D. degree, under Grant CSC201908350102. This article was presented in part at the Conference IEEE International Symposium on Wireless Personal Multimedia Communications (WPMC), Bali, November 2017. The associate editor coordinating the review of this article and approving it for publication was W. P. Tay. *(Corresponding author: Rui Zhao.)*

Yuanjian Li, Yansha Deng, and A. Hamid Aghvami are with the Centre for Telecommunications Research (CTR), King's College London, London WC2R 2LS, U.K. (e-mail: yuanjian.li@kcl.ac.uk; yansha.deng@kcl.ac.uk; hamid.aghvami@kcl.ac.uk).

Rui Zhao is with the Xiamen Key Laboratory of Mobile Multimedia Communications, Huaqiao University, Xiamen 361021, China (e-mail: rzhao@hqu.edu.cn).

Feng Shu is with the School of Information and Communication Engineering, Hainan University, Haikou 570228, China, and also with the School of Electronic and Optical Engineering, Nanjing University of Science and Technology, Nanjing 210094, China (e-mail: shufeng0101@163.com).

Zhiqiao Nie is with the Xiamen Meiya Pico Information Company, Ltd., Xiamen 361008, China (e-mail: zhqnie@163.com).

Color versions of one or more of the figures in this article are available online at https://ieeexplore.ieee.org.

Digital Object Identifier 10.1109/TWC.2020.3015816

I. Introduction

INSPIRED by the fact that radio frequency (RF) signals can carry information and energy at the same time, the concept of simultaneous wireless information and power transfer (SWIPT) was coined in [2]. Thereafter, two practical SWIPT strategies were introduced in [3], i.e., time-switching (TS) and power-splitting (PS) based SWIPT, in which information decoding (ID) and energy harvesting (EH) are conducted in time or power domain, respectively [4]. Universally, PS-based SWIPT can gain more spectral efficiency (SE) compared with TS-based counterpart, via consuming less time slots. SWIPT techniques have been successfully utilised in power-limited wireless devices, releasing more deployment flexibility for wireless transceivers from power cables [5]–[7]. One popular SWIPT application is SWIPT-aided relaying networks, which can not only solve power supply problem for energy-limited relay, but also take advantages of information-energy trade-off. However, most existing works on SWIPT-assisted relaying networks are constrained to half-duplex (HD) relay, theoretically resulting in 50% SE loss. Full-duplex (FD) technology, which allows transceivers emit and receive information simultaneously, can potentially achieve efficient utilization of wireless resources (i.e., time and frequency), and thus it is expected to overcome the shortcomings of HD counterpart on SE [8], [9]. Therefore, lots of research have been devoted to integrate FD relaying (FDR) techniques into PS-based SWIPT to overcome energy deficiency and enhance the utilization efficiency of wireless resources [10], [11]. Wang *et al.* [10] investigated characteristics and performance of PS-based two-way SWIPT FDR networks as well as the relay selection issue. Liu *et al.* [11] examined the outage probability and average throughput performances in a PS-based SWIPT FDR wireless network.

Unfortunately, the inherently public and visible nature of wireless medium (electromagnetic wave) leads to privacy weakness, i.e., the existence of wireless interactions can be detected easily, which is an overlooked but critical issue in the field of wireless communications. Recently, increasing research efforts have been devoted to low probability of detection, namely, covert communications, aiming at hiding wireless transmissions from being detected by a warden [12], [13]. The famous Square Root Law, which indicates the fact that $\mathcal{O}(\sqrt{n})$ bits of information can be transmitted reliably and covertly in n channel uses over additive white Gaussian

noise (AWGN) channels as $n \to +\infty$, was initiated in [14]. Besides, Goeckel *et al.* [15] proved that it is possible for the transmitter to covertly send $\mathcal{O}(\sqrt{n})$ bits to the intended receiver, when the warden has no exact knowledge of its noise power. Additionally, covert communication problems have been studied in the field of wireless relaying networks [16]–[18]. Hu *et al.* [16] examined the possibility, performance limits, and associated costs for a power-constrained HD relay transmitting covert information on top of forwarding the source's information. The possibility and achievable performance of low probability of detection in on-way HD relay system were examined in [17], in which rate-control and power-control transmission strategies were considered, respectively. Wang *et al.* [18] investigated how channel uncertainty can influence covert communication performance in wireless relaying networks.

Note that the aforementioned research on SWIPT FDR mainly considered fixed working mode of the FD relay, which severely restricts the flexibility and efficiency of wireless energy manipulation and information forwarding. Meanwhile, the majority of studies on SWIPT applies continuous EH assumptions without considering the impact of energy accumulation, which may lead to insufficient power supply. Additionally, covert communication problems have been seldom considered in the FD relay networks, potentially resulting in sensitive information leakage if the relay node is malicious. Motivated by the aforementioned contents, we propose a novel SWIPT FDR protocol termed as harvest-and-opportunistically-relay (HOR), in which we consider adaptive relay working mode, practical energy accumulation and discrete EH technique as well as covert communications, aiming at enhancing wireless energy manipulating efficiency and wireless transmission performance, while improving its privacy level. The main contributions of the article are concluded in details as follows.

- *Hybrid Energy Storage and Markov Chain*: To truly enable the relay's FD functionality, a hybrid energy storage scheme is adopted. To track dynamic fluctuation of residual energy, energy discretization and discrete-state MC method are applied to model the complicated energy state transitions. All the transition probabilities are calculated in closed-form, which facilitates the derivation of the MC's stationary distribution.
- *Covert Communication Analysis*: We provide covert communication analysis under channel uncertainty and the optimality of radiometer for covert message detection is proved. Closed-form expressions of false alarm and missed detection probabilities are derived, based on which we calculate closed-form expressions of the optimal detection threshold and the corresponding minimum detection error probability. Numerical results show that the optimal detection threshold can help achieve a better covert transmission detection performance, which enhances the privacy level of our proposed HOR protocol. Furthermore, the impact of imperfect channel estimation on the minimum detection error probability is discussed.
- *Transmission Performance Analysis*: Invoking the MC's stationary distribution, closed-form expression of transmission outage probability is derived, then we provide transmission outage analysis of the proposed HOR scheme. Furthermore, the impacts of key system parameters on transmission outage performance are investigated via numerical results.

Organization: Section II presents the HOR model and its transmission strategy. Section III describes the energy discretization, the MC and the stationary distribution. Section IV shows covert communication analysis. Section V gives transmission outage performance analysis. Simulation results are presented in Section VI and conclusions are drawn in Section VII.

II. System Model and Transmission Strategy

A classical three-node wireless relaying network, which comprises one source (S), one destination (D) and one relay (R), is considered.[1] Energy-constrained R is equipped with two antennas so that it can adopt the FD technique, whereas S and D are both single-antenna node. A novel HOR protocol is proposed to assist wireless communication from S to D with the ability of managing RF energy smartly, while improving the overall privacy level.

A. Assumptions Regarding Wireless Channels

Note that all wireless channels are assumed to follow the quasi-static Rayleigh fading,[2] and the block boundaries in wireless links are predefined to be synchronized perfectly. Without loss of generality, the block duration in the considered scenario is normalized to one time unit so that the measures of power and energy are identical and can be used interchangeably. Wireless channels S→D, S→R, and R→D are denoted as h_{SD}, h_{SR}, and h_{RD}, respectively. Moreover, h_{RR} indicates the SI link at R.[3] All wireless channel coefficients follow independently and identically distributed (i.i.d.) complex Gaussian distribution with zero means and variances $\mathbb{E}\left\{|h_{\mathrm{SD}}|^2\right\} = \Omega_{\mathrm{SD}}$, $\mathbb{E}\left\{|h_{\mathrm{SR}}|^2\right\} = \Omega_{\mathrm{SR}}$, $\mathbb{E}\left\{|h_{\mathrm{RD}}|^2\right\} = \Omega_{\mathrm{RD}}$ and $\mathbb{E}\left\{|h_{\mathrm{RR}}|^2\right\} = \Omega_{\mathrm{RR}}$.

We assume that the instantaneous channel state information (CSI) of channel between S and D can be available at S via channel estimation, but D can only gain the imperfect instantaneous CSI estimation of the channel

[1] It is worth extending our three-node model to multiple nodes scenario for gaining more comprehensive insights, which is a subject of our future research.

[2] The Rayleigh fading distribution that the self-interference (SI) channel at R follows is considered because the line-of-sight (LoS) component can be largely eliminated via antenna isolation and the scattering plays the principal role herein.

[3] It is worth noting that the channel coefficients h_{SD}, h_{SR}, h_{RD} and h_{RR} are manipulated to encompass the gains of transmit and receive antennas as well as the path losses cased by propagation distances among the nodes, for the sake of conciseness.

between R and D.[4] We note hereby that the availability of instantaneous S→R and R→R CSIs poses no influence on the considered performance analyses so that we do not rise any assumption on their availabilities.

B. Relay Model

In the considered system, R is known publicly as an energy-limited device. To efficiently solve power supply problem, different from conventional fixed-mode FDR scheme, a novel FDR protocol termed as HOR is initiated, which allows R to work in either the pure EH (PEH) mode or the FD SWIPT mode opportunistically. In specific, when performing the FD SWIPT, R receives and forwards information simultaneously assisting the wireless transmission between S and D, while the PS-based EH solution is applied to harvest the RF energy. When adopting the PEH mode, R concentrates on capturing wireless energy without information processing.

Alongside assisting signal transmission, R may leak essential information (defined as the covert message herein) regarding the source signals. The legal destination D also plays the role as a *warden* detecting the potential information leakage. To reduce the probability of being detected by the legitimate party, R prefers to emit the covert message under solid covers. In this proposed system, the forwarded version of the source signals is the only existing cover. Reasonably, R would intend to broadcast the covert message merely when itself works in the FD SWIPT mode. Otherwise, the covert messages initiated by R will be detected by D with relatively high probability. This is because, when the PEH is active, R is supposed to focus on EH without forwarding and any additional transmit power will be detected easily by D.

To achieve the proposed HOR functionality, R should equip the following hardwares: 1) three RF chains, enabling the EH, information forwarding and covert message emitting; 2) one rectifier utilized to transform the RF signals into direct currents (DC); 3) a battery serving as the principal energy carrier (PEC) with high energy capacity; 4) one minor battery (MB) for storing harvested energy temporarily, e.g., a capacitor; 5) a constant energy supply exclusively for sending covert message, whose existence is unaware publicly.

Specifically, the receive antenna at R is permanently bounded with the rectifier via one RF chain. One single battery cannot be charged and discharged simultaneously so that the FD SWIPT mode may not be truly realised, we herein apply the hybrid energy storage method to resolve this dilemma. Note that the PEC is directly connected to the rectifier and the broadcasting RF chain for absorbing and releasing energy, respectively. In the PEH mode, the harvested energy are assimilated by the PEC directly. Otherwise, the PEC releases its residual energy to support the broadcasting RF chain. Meanwhile, the MB stores the harvested energy temporarily and delivers all the stored energy into the PEC once the FD SWIPT mode terminates. The hidden constant energy supply connected to the 3rd RF chain will release its power only when R decides to leak.

[4]The instantaneous CSI of channel between S and D is gained via the minimum mean square error (MMSE) channel estimation technique and feedback link. Specifically, D applies the MMSE method to estimate channel S → D and then sends the estimated CSI to S via an ideal feedback link. Here, we assume that D can estimate channel S → D with negligible estimation error. To make the HOR system more practical and leave space to analyze the impact of imperfect channel estimation on covert communication performance, we focus on the circumstance in which D can only obtain imperfect CSI of channel R → D.

C. Transmission Protocol

In our proposed HOR protocol, at the beginning of each transmission block, S broadcasts pilot signal to estimate h_{SD}, which will be utilized to calculate the received instantaneous signal-to-noise-ratio (SNR) at D, i.e., $\gamma_{\mathrm{SD}} = P_{\mathrm{S}} |h_{\mathrm{SD}}|^2 / \sigma_{\mathrm{D}}^2$. Here, P_{S} represents average transmit power at S and σ_{D}^2 is the power of additive white Gaussian noise (AWGN) at D. In the case of $\gamma_{\mathrm{SD}} \geq \gamma_{th}$, D feeds back two bits "11" to S through a feedback link, where γ_{th} is a predefined instantaneous SNR threshold. Otherwise, D feeds back two bits "00" instead. When S receives the feedback bits "11", S broadcasts two bits "01" to R. Otherwise (i.e., S receives "00"), S sends out bits "10" alternatively. If R receives "01", it means the direct link between S and D is good enough so that R is not necessarily needed to assist the transmission and R keeps working in the PEH mode without forwarding any information (of course, including the possible covert message). If R receives bits "10", which means the quality of received information at D is poor, R is expected to help the transmission from S to D. Before participating in transmission, R has to estimate its residual energy, to determine whether the available energy is sufficient to support the transmission. If the energy state of R is greater than a given residual energy threshold E_{th}, i.e., $E_i \geq E_{th}$, R feeds back bit "1" to S, otherwise, feeds back bit "0" instead. Once S receives the feedback bit "1" from R, S starts to broadcast the intended information signal, and R turns into the FD SWIPT mode, i.e., R helps S forward the information signal and harvests energy simultaneously. If S receives the feedback bit "0" from R, S broadcasts energy signal to charge the battery at R. At this moment, D ceases signal processing, because the energy signal is randomly generated by S and conveys no useful information. The condition $\gamma_{\mathrm{SD}} \geq \gamma_{th}$ is referred to the "SNR requirement" which is applied to guarantee the reliability of communication from S to D. On the other hand, the condition $E_i \geq E_{th}$ is regarded as the "energy requirement", ensuring that the residual energy at R is sufficient to support the relaying work.

1) The PEH Mode: Note that the PEH mode will be enabled in the case of either $\gamma_{\mathrm{SD}} \geq \gamma_{th}$ or $\{\gamma_{\mathrm{SD}} < \gamma_{th}\} \cap \{E_i < E_{th}\}$. By ignoring the negligible energy harvested from the noise at the receiver, the total amount of energy harvested at R in a transmission slot can be given by

$$E_{\mathrm{PEH}} = \eta P_{\mathrm{S}} |h_{\mathrm{SR}}|^2, \tag{1}$$

where $\eta\,(0 < \eta < 1)$ means the efficiency of energy conversion, and the harvested energy in this stage will be straight transferred into the PEC.

2) The FD SWIPT Mode: It is worth noting that the FD SWIPT mode will be invoked when the case $\{\gamma_{\mathrm{SD}} < \gamma_{th}\} \cap \{E_i \geq E_{th}\}$ holds. Only in this circumstance, R gets chance to broadcast covert message under the shield of the forwarded source signals.

When R does not leak, the received signals at R and D can be expressed as

$$\boldsymbol{y}_{\mathrm{R}}[\omega] = \sqrt{P_{\mathrm{S}}}h_{\mathrm{SR}}\boldsymbol{x}_{\mathrm{S}}[\omega] + \sqrt{kP_{\mathrm{R}}}h_{\mathrm{RR}}\boldsymbol{x}_{\mathrm{R}}[\omega] + \boldsymbol{n}_{\mathrm{R}}[\omega], \quad (2)$$

$$\boldsymbol{y}_{\mathrm{D}}[\omega] = \sqrt{P_{\mathrm{S}}}h_{\mathrm{SD}}\boldsymbol{x}_{\mathrm{S}}[\omega] + \sqrt{P_{\mathrm{R}}}h_{\mathrm{RD}}\boldsymbol{x}_{\mathrm{R}}[\omega] + \boldsymbol{n}_{\mathrm{D}}[\omega], \quad (3)$$

respectively, where P_{R} means average transmit power at R, $\boldsymbol{x}_{\mathrm{S}}[\omega] \sim \mathcal{CN}(0,1)$ represents the intended signal emitted from S, $\omega \in \{1,2,\ldots,n\}$ denotes the symbol index in a transmission block and n measures the block-length. $\boldsymbol{x}_{\mathrm{R}}[\omega] = \boldsymbol{x}_{\mathrm{S}}[\omega - \eth]$ is the forwarded version of $\boldsymbol{x}_{\mathrm{S}}[\omega - \eth]$ after decoding and recoding, where $\boldsymbol{x}_{\mathrm{R}}[\omega] \sim \mathcal{CN}(0,1)$ and integer $\eth$ represents the number of delayed symbols due to signal processing. The AWGNs received at R and D are marked as $\boldsymbol{n}_{\mathrm{R}}$ and $\boldsymbol{n}_{\mathrm{D}}$, with $\boldsymbol{n}_{\mathrm{R}}[\omega] \sim \mathcal{CN}\left(0,\sigma_{\mathrm{R}}^2\right)$ and $\boldsymbol{n}_{\mathrm{D}}[\omega] \sim \mathcal{CN}\left(0,\sigma_{\mathrm{D}}^2\right)$, respectively. Here, we consider a practical scenario where imperfect SI cancellation (SIC) assumption is adopted, and the variable $k \in (0,1]$ represents the SIC coefficient implying different SIC levels.

When R decides to leak, the received signals at R and D can be expressed as

$$\begin{aligned}\boldsymbol{y}_{\mathrm{R}}[\omega] = {} & \sqrt{P_{\mathrm{S}}}h_{\mathrm{SR}}\boldsymbol{x}_{\mathrm{S}}[\omega] + \sqrt{kP_{\mathrm{R}}}h_{\mathrm{RR}}\boldsymbol{x}_{\mathrm{R}}[\omega] \\ & + \sqrt{kP_{\Delta}}h_{\mathrm{RR}}\boldsymbol{x}_{\mathrm{c}}[\omega] + \boldsymbol{n}_{\mathrm{R}}[\omega], \quad (4)\\ \boldsymbol{y}_{\mathrm{D}}[\omega] = {} & \sqrt{P_{\mathrm{S}}}h_{\mathrm{SD}}\boldsymbol{x}_{\mathrm{S}}[\omega] + \sqrt{P_{\mathrm{R}}}h_{\mathrm{RD}}\boldsymbol{x}_{\mathrm{R}}[\omega] \\ & + \sqrt{P_{\Delta}}h_{\mathrm{RD}}\boldsymbol{x}_{\mathrm{c}}[\omega] + \boldsymbol{n}_{\mathrm{D}}[\omega], \quad (5)\end{aligned}$$

respectively, where P_{Δ} means average transmit power of covert message $\boldsymbol{x}_{\mathrm{c}}$ with $\boldsymbol{x}_{\mathrm{c}}[\omega] \sim \mathcal{CN}(0,1)$. Note that P_{Δ} merely comes from the constant energy supply.

To enable the FD SWIPT mode, the PS-based EH protocol is adopted. Specifically, R splits the power of received signal into $\rho : (1-\rho)$ proportions. The ρ portion of the received signal power is used to EH and the remaining $(1-\rho)$ portion is allocated to information processing. Therefore, after ignoring the negligible energy harvested form the AWGN, the energy harvested at R in each time slot can be calculated as $E_{\mathrm{FS0}} = \eta\rho(P_s|h_{\mathrm{SR}}|^2 + kP_{\mathrm{R}}|h_{\mathrm{RR}}|^2)$ or $E_{\mathrm{FS1}} = \eta\rho(P_s|h_{\mathrm{SR}}|^2 + kP_{\mathrm{R}}|h_{\mathrm{RR}}|^2 + kP_{\Delta}|h_{\mathrm{RR}}|^2)$, where the subscript "FS0" refers to the FD SWIPT mode without sending covert message, another subscript "FS1" means the FD SWIPT mode with covert message. Particularly, we constrain the total transmit power at R in the FD SWIPT mode as $P_{\mathrm{FS0}} = P_{\mathrm{R}}$ and $P_{\mathrm{FS1}} = P_{\mathrm{R}} + P_{\Delta}$, respectively. Hence, the harvested energy can be reconstructed uniformly as

$$E_{\mathrm{FS}} = \eta\rho\left(P_s|h_{\mathrm{SR}}|^2 + kP_{\mathrm{FS}}|h_{\mathrm{RR}}|^2\right), \quad (6)$$

where $P_{\mathrm{FS}} \in \{P_{\mathrm{FS0}}, P_{\mathrm{FS1}}\}$ and $E_{\mathrm{FS}} \in \{E_{\mathrm{FS0}}, E_{\mathrm{FS1}}\}$.

III. Markov Chain and Stationary Distribution

The hybrid energy container makes R possible to absorb and release energy at the same time. However, it also leads to highly complex and dynamic charge-discharge behaviours at R, which poses solid obstacle for tracking energy state changes mathematically. To tackle this problem, the MC-based method is invoked to track the complex energy transmission procedure.

A. Energy Discretization

To describe the dynamic charge-discharge behaviours of the PEC, we need to discretize the battery capacity into discrete energy states. Each energy state implies the available energy remained in the PEC, which can be reached by calculating the product of the corresponding number of energy levels and the unit energy level. In details, the PEC is quantized into $L+1$ states, and the unit energy level is equal to C_{P}/L where C_{P} represents the energy capacity of the PEC. Therefore, the i-th energy state is defined as $E_i = iC_{\mathrm{P}}/L, i \in \{0,1,\ldots,L\}$.[5] Note that $C_{\mathrm{P}} \geq E_{th}$ is considered, otherwise R gets no opportunity to work in the FD SWIPT mode. In the PEH mode, the discretized amount of energy absorbed by the PEC is derived as

$$\Xi_{\mathrm{PEH}} \triangleq \left\lfloor \frac{E_{\mathrm{PEH}}}{C_{\mathrm{P}}/L} \right\rfloor \frac{C_{\mathrm{P}}}{L} = \frac{q_{\mathrm{PEH}}C_{\mathrm{P}}}{L}, \quad (7)$$

where $\lfloor\cdot\rfloor$ denotes the floor function and $q_{\mathrm{PEH}} \in \{1,2,\ldots,L\}$. Without loss of generality, we declare that the i-th energy state represents the initial energy amount available in the PEC. After energy-absorbing in the PEH mode, if $E_i + \Xi_{\mathrm{PEH}} \geq C_{\mathrm{P}}$, the PEC will be charged to the maximal capacity $E_L = C_{\mathrm{P}}$ and any overflowed energy has to be abandoned. Otherwise, the latest energy state is $E_{i+q_{\mathrm{PEH}}} = E_i + \Xi_{\mathrm{PEH}}$ which is guaranteed to be fully accommodated by the PEC.

Because the MB is subject to a predefined energy capacity C_{M}, the potential amount of energy transferred into the PEC should be reasonably constrained by $\min\{E_{\mathrm{FS}}, C_{\mathrm{M}}\}$ where the function $\min\{x,y\}$ outputs the smaller value. Practically, energy transfer from the MB to the PEC suffers from circuitry attenuation. Thus, the actual amount of energy absorbed by the PEC can be given by $\hat{E}_{\mathrm{FS}} = \eta' \times \min\{E_{\mathrm{FS}}, C_{\mathrm{M}}\}$, where η' denotes the circuitry attenuation coefficient. Furthermore, the discretized amount of energy absorbed by the PEC should be expressed as

$$\Xi_{\mathrm{FS}} \triangleq \left\lfloor \frac{\hat{E}_{\mathrm{FS}}}{C_{\mathrm{P}}/L} \right\rfloor \frac{C_{\mathrm{P}}}{L} = \frac{q_{\mathrm{FS}}C_{\mathrm{P}}}{L}, \quad (8)$$

where $q_{\mathrm{FS}} \in \{1,2,\ldots,L\}$. Invoking the energy requirement, the consumed energy for forwarding information should locate at $E_{\mathrm{FS}}^{\mathrm{C}} \in [E_{th}, E_i]$, where we set $E_{\mathrm{FS}}^{\mathrm{C}} = P_{\mathrm{R}} = E_{th} = 0.6C_{\mathrm{P}}$ for simplicity. After discretization, the amount of energy consumption at the PEC can be given by

$$\Xi_{\mathrm{FS}}^{\mathrm{C}} = \left\lceil \frac{E_{\mathrm{FS}}^{\mathrm{C}}}{C_{\mathrm{P}}/L} \right\rceil \frac{C_{\mathrm{P}}}{L} = \frac{q_{\mathrm{FS}}^{\mathrm{C}}C_{\mathrm{P}}}{L}, \quad (9)$$

where $\lceil\cdot\rceil$ stands as the ceiling function, and $q_{\mathrm{FS}}^{\mathrm{C}}$ is defined for notation simplicity. Similarly, if $E_i - \Xi_{\mathrm{FS}}^{\mathrm{C}} + \Xi_{\mathrm{FS}} \geq C_1$, the PEC will be fully charged to $E_L = C_{\mathrm{P}}$. On the contrary, the latest energy state after charging is $E_{i-q_{\mathrm{FS}}^{\mathrm{C}}+q_{\mathrm{FS}}} = E_i - \Xi_{\mathrm{FS}}^{\mathrm{C}} + \Xi_{\mathrm{FS}}$.

[5] In the case of infinite energy discretization, i.e., $L \to +\infty$, the proposed discrete battery model can tightly track the behavior of continuous linear battery which is widely applied in the literature.

B. Markov Chain

Following the energy discretization, we are able to track the transition procedure of energy states at the PEC among multiple transmission blocks as a finite-state time-homogeneous MC. The transition probability $p_{i,j}$ denotes the probability of energy state transition from E_i to E_j, which occurs between the beginning of a transmission block and that of the next transmission block. The energy state transitions can be stated comprehensively in the following six cases.

1) From E_0 to E_0: In this case, R cannot afford the FD SWIPT mode. After a transmission block, the residual energy yet remains empty. It indicates that the total harvested energy in this PEH block is discretized to zero, namely, $\Xi_{\text{PEH}} = 0$. Invoking (1) and (7), the transition probability of $E_0 \to E_0$ can be given by $p_{0,0} = \Pr(q_{\text{PEH}} = 0) = \Pr[|h_{\text{SR}}|^2 < C_{\text{P}}/(\eta P_{\text{S}} L)]$. Since $|h_{\text{SR}}|^2$ follows the exponential distribution with mean Ω_{SR}, the cumulative distribution function (CDF) of $|h_{\text{SR}}|^2$ is given by $F_{|h_{\text{SR}}|^2}(x) = 1 - \exp(-x/\Omega_{\text{SR}})$. Furthermore, we get $p_{0,0} = F_{|h_{\text{SR}}|^2}[C_{\text{P}}/(\eta P_{\text{S}} L)]$.

2) From E_L to E_L: In this case, whether R works in the PEH mode or the FD SWIPT mode depends merely on the SNR requirement. If the PEH mode is invoked, the harvested energy can be any possible value, since the PEC cannot absorb additional energy. If the FD SWIPT mode is activated, the consumed energy should be less than or equal to its harvested counterpart. From (6), (8) and (9), the transition probability of $E_L \to E_L$ can be shown as $p_{L,L} = \Pr(\gamma_{\text{SD}} \geq \gamma_{th}) + \Pr(\gamma_{\text{SD}} < \gamma_{th}) \Pr\left(\Xi_{\text{FS}}^{\text{C}} \leq \Xi_{\text{FS}}\right)$. Similar to Case 1), we can obtain $q_{\text{SD}} = \Pr(\gamma_{\text{SD}} < \gamma_{th}) = F_{|h_{\text{SD}}|^2}\left(\sigma_{\text{D}}^2 \gamma_{th}/P_{\text{S}}\right)$ and $\Pr(\gamma_{\text{SD}} \geq \gamma_{th}) = 1 - F_{|h_{\text{SD}}|^2}\left(\sigma_{\text{D}}^2 \gamma_{th}/P_{\text{S}}\right) = 1 - q_{\text{SD}}$. Regarding $\Pr\left(\Xi_{\text{FS}}^{\text{C}} \leq \Xi_{\text{FS}}\right)$, we obtain

$$\begin{aligned}\Pr\left(\Xi_{\text{FS}}^{\text{C}} \leq \Xi_{\text{FS}}\right) &= \Pr\left[\left(q_{\text{FS}}^{\text{C}} \leq \frac{\eta' E_{\text{FS}}}{C_{\text{P}}/L}\right) \bigcap (E_{\text{FS}} < C_{\text{M}})\right] \\ &\quad + \Pr\left[\left(q_{\text{FS}}^{\text{C}} \leq \frac{\eta' C_{\text{M}}}{C_{\text{P}}/L}\right) \bigcap (E_{\text{FS}} \geq C_{\text{M}})\right] \\ &= \begin{cases} \Pr\left(E_{\text{FS}} \geq \dfrac{q_{\text{FS}}^{\text{C}} C_{\text{P}}}{\eta' L}\right), & C_{\text{M}} \geq \dfrac{q_{\text{FS}}^{\text{C}} C_{\text{P}}}{\eta' L} \\ 0, & C_{\text{M}} < \dfrac{q_{\text{FS}}^{\text{C}} C_{\text{P}}}{\eta'\ L}. \end{cases}\end{aligned} \tag{10}$$

Invoking (6), we gain $\Pr\left[E_{\text{FS}} \geq q_{\text{FS}}^{\text{C}} C_{\text{P}}/(\eta' L)\right] = \Pr\left[Z \geq q_{\text{FS}}^{\text{C}} C_{\text{P}}/(\eta\rho\eta' L)\right]$, where $Z = P_s |h_{\text{SR}}|^2 + k P_{\text{FS}} |h_{\text{RR}}|^2$. Via convolution of two exponential distribution variables, we obtain the CDF of Z as

$$\begin{aligned}&F_Z(x) \\ &= \begin{cases} 1 - \dfrac{P_{\text{S}}\Omega_{\text{SR}}}{P_{\text{S}}\Omega_{\text{SR}} - k P_{\text{FS}}\Omega_{\text{RR}}} e^{-\frac{x}{P_{\text{S}}\Omega_{\text{SR}}}} \\ \quad + \dfrac{k P_{\text{FS}}\Omega_{\text{RR}}}{P_{\text{S}}\Omega_{\text{SR}} - k P_{\text{FS}}\Omega_{\text{RR}}} e^{-\frac{x}{k P_{\text{FS}}\Omega_{\text{RR}}}}, & P_{\text{S}}\Omega_{\text{SR}} \neq k P_{\text{FS}}\Omega_{\text{RR}} \\ \frac{1}{2}\gamma\left(2, \dfrac{x}{P_{\text{S}}\Omega_{\text{SR}}}\right), & P_{\text{S}}\Omega_{\text{SR}} = k P_{\text{FS}}\Omega_{\text{RR}}, \end{cases}\end{aligned} \tag{11}$$

where $\gamma(\cdot,\cdot)$ is the lower incomplete Gamma function. Furthermore, we get $\Pr\left[E_{\text{FS}} \geq q_{\text{FS}}^{\text{C}} C_{\text{P}}/(\eta' L)\right] = 1 - F_Z\left[q_{\text{FS}}^{\text{C}} C_{\text{P}}/(\eta\rho\eta' L)\right]$. Finally, we can obtain

$$p_{L,L} = \begin{cases} 1 - q_{\text{SD}} F_Z\left(\dfrac{q_{\text{FS}}^{\text{C}} C_{\text{P}}}{\eta\rho\eta' L}\right), & C_{\text{M}} \geq \dfrac{q_{\text{FS}}^{\text{C}} C_{\text{P}}}{\eta' L} \\ 1 - q_{\text{SD}}, & C_{\text{M}} < \dfrac{q_{\text{FS}}^{\text{C}} C_{\text{P}}}{\eta' L}. \end{cases} \tag{12}$$

3) From E_i to E_j $(0 \leq i < j < L)$: If the initial energy state cannot satisfy the energy requirement, i.e., $E_i < E_{th}$, the PEH mode will be selected. Otherwise, when $\gamma_{\text{SD}} \geq \gamma_{th}$, R will choose the PEH mode. On the contrary, R will work in the FD SWIPT mode. Thus, the transition probability of $E_i \to E_j$ can be expressed as

$$\begin{aligned} p_{i,j} &= q_{\text{SD}} \Pr(E_i < E_{th}) \Pr(q_{\text{PEH}} = j - i) \\ &\quad + q_{\text{SD}} \Pr(E_i \geq E_{th}) \Pr\left(q_{\text{FS}} - q_{\text{FS}}^{\text{C}} = j - i\right) \\ &\quad + (1 - q_{\text{SD}}) \Pr(q_{\text{PEH}} = j - i) \\ &= \begin{cases} \Pr(q_{\text{PEH}} = j - i), & i < \varphi \\ (1 - q_{\text{SD}}) \Pr(q_{\text{PEH}} = j - i) & \\ \quad + q_{\text{SD}} \Pr\left(q_{\text{FS}} - q_{\text{FS}}^{\text{C}} = j - i\right), & i \geq \varphi, \end{cases} \end{aligned} \tag{13}$$

where $\varphi = \lceil E_{th} L/C_{\text{P}} \rceil$ denotes the total number of energy units needed to represent the energy requirement in the discretized energy regime. Next, we calculate $\Pr(q_{\text{PEH}} = j - i)$ and $\Pr\left(q_{\text{FS}} - q_{\text{FS}}^{\text{C}} = j - i\right)$, shown respectively as (14) and (15) in the following.

$$\begin{aligned} &\Pr(q_{\text{PEH}} = j - i) \\ &= F_{|h_{\text{SR}}|^2}\left[\frac{(j - i + 1) C_{\text{P}}}{\eta P_{\text{S}} L}\right] - F_{|h_{\text{SR}}|^2}\left[\frac{(j - i) C_{\text{P}}}{\eta P_{\text{S}} L}\right]. \end{aligned} \tag{14}$$

$$\begin{aligned} &\Pr\left(q_{\text{FS}} - q_{\text{FS}}^{\text{C}} = j - i\right) \\ &= \begin{cases} 0, & C_{\text{M}} < \dfrac{(j - i + q_{\text{FS}}^{\text{c}}) C_{\text{P}}}{\eta' L} \\ F_Z\left[\dfrac{(j - i + q_{\text{FS}}^{\text{c}} + 1) C_{\text{P}}}{\eta\rho\eta' L}\right] & \\ \quad - F_Z\left[\dfrac{(j - i + q_{\text{FS}}^{\text{c}}) C_{\text{P}}}{\eta\rho\eta' L}\right], & C_{\text{M}} \geq \dfrac{(j - i + q_{\text{FS}}^{\text{c}} + 1) C_{\text{P}}}{\eta' L} \\ 1 - F_Z\left[\dfrac{(j - i + q_{\text{FS}}^{\text{c}}) C_{\text{P}}}{\eta\rho\eta' L}\right], & \text{otherwise.} \end{cases} \end{aligned} \tag{15}$$

Combining (13), (14) and (15), we obtain the probability of transition $E_i \to E_j$ as (16), shown at the bottom of the next page.

4) From E_i to E_i $(0 < i < L)$: If $E_i < E_{th}$, the PEH mode will be invoked and the harvested energy should be discretized as zero. If $E_i \geq E_{th}$ and $\gamma_{\text{SD}} \geq \gamma_{th}$, the PEH mode is enabled and the harvested energy should also be discretized as zero. If $E_i \geq E_{th}$ and $\gamma_{\text{SD}} < \gamma_{th}$, the FD SWIPT mode will be selected, the discretized amount of consumed energy should be equal to that of harvested energy. Hence, the transition

probability of $E_i \to E_i$ is calculated as

$$\begin{aligned} p_{i,i} &= (1-q_{\text{SD}})\Pr(q_{\text{PEH}}=0)+q_{\text{SD}}\Pr(E_i<E_{th})\Pr(q_{\text{PEH}}=0) \\ &\quad + q_{\text{SD}}\Pr\left(E_i \geq E_{th}\right)\Pr\left(q_{\text{FS}}-q_{\text{FS}}^{\text{C}}=0\right) \\ &= \begin{cases} \Pr\left(q_{\text{PEH}}=0\right), & i<\varphi \\ (1-q_{\text{SD}})\Pr\left(q_{\text{PEH}}=0\right) & \\ \quad + q_{\text{SD}}\Pr\left(q_{\text{FS}}-q_{\text{FS}}^{\text{C}}=0\right), & i \geq \varphi, \end{cases} \end{aligned} \tag{17}$$

where

$$\begin{aligned} &\Pr\left(q_{\text{FS}}-q_{\text{FS}}^{\text{C}}=0\right) \\ &= \begin{cases} 0, & C_{\text{M}} < \dfrac{q_{\text{FS}}^{\text{c}} C_{\text{P}}}{\eta' L} \\ F_Z\left[\dfrac{\left(q_{\text{FS}}^{\text{c}}+1\right)C_{\text{P}}}{\eta\rho\eta' L}\right] & \\ \quad - F_Z\left(\dfrac{q_{\text{FS}}^{\text{c}} C_{\text{P}}}{\eta\rho\eta' L}\right), & C_{\text{M}} \geq \dfrac{\left(q_{\text{FS}}^{\text{c}}+1\right)C_{\text{P}}}{\eta' L} \\ 1-F_Z\left(\dfrac{q_{\text{FS}}^{\text{c}} C_{\text{P}}}{\eta\rho\eta' L}\right), & \text{otherwise.} \end{cases} \end{aligned} \tag{18}$$

Finally, we get the transition probability of $E_i \to E_i$ as (19), shown at the bottom of the page.

5) From E_i to E_j $(0 \leq j < i \leq L)$: Obviously, this circumstance can only occur in the FD SWIPT mode. Therefore, the transition probability of $E_i \to E_j$ can be derived as

$$\begin{aligned} p_{i,j} &= \Pr\left(\gamma_{\text{SD}} < \gamma_{th}\right)\Pr\left(E_i \geq E_{th}\right)\Pr\left(q_{\text{FS}}^{\text{C}}-q_{\text{FS}}=i-j\right) \\ &= \begin{cases} 0, & i<\varphi \\ q_{\text{SD}}\Pr\left(q_{\text{FS}}^{\text{C}}-q_{\text{FS}}=i-j\right), & i \geq \varphi. \end{cases} \end{aligned} \tag{20}$$

Next, we need to calculate $\Pr\left(q_{\text{FS}}^{\text{C}}-q_{\text{FS}}=i-j\right)$, shown as

$$\begin{aligned} &\Pr\left(q_{\text{FS}}^{\text{C}}-q_{\text{FS}}=i-j\right) \\ &= \begin{cases} 0, & C_{\text{M}} < \dfrac{\left[q_{\text{FS}}^{\text{C}}-(i-j)\right]C_{\text{P}}}{\eta' L} \\ F_Z\left(\dfrac{\left[q_{\text{FS}}^{\text{C}}-(i-j)+1\right]C_{\text{P}}}{\eta\rho\eta' L}\right) & \\ \quad - F_Z\left(\dfrac{\left[q_{\text{FS}}^{\text{C}}-(i-j)\right]C_{\text{P}}}{\eta\rho\eta' L}\right), & C_{\text{M}} \geq \dfrac{\left[q_{\text{FS}}^{\text{C}}-(i-j)+1\right]C_{\text{P}}}{\eta' L} \\ 1-F_Z\left(\dfrac{\left[q_{\text{FS}}^{\text{C}}-(i-j)\right]C_{\text{P}}}{\eta\rho\eta' L}\right), & \text{otherwise.} \end{cases} \end{aligned} \tag{21}$$

Invoking (20) and (21), we can express the transition probability of $E_i \to E_j$ as (22), shown at the bottom of the next page.

6) From E_i to E_L $(0 \leq i < L)$: When $E_i < E_{th}$, the PEH mode will be activated, and the harvested energy should meet $\Xi_{\text{PEH}} \geq E_L - E_i$. Otherwise, if $\gamma_{\text{SD}} \geq \gamma_{th}$, the PEH is invoked and the harvested energy is supposed to satisfy $\Xi_{\text{PEH}} \geq E_L - E_i$. If $E_i \geq E_{th}$ and $\gamma_{\text{SD}} < \gamma_{th}$, the FD SWIPT mode will

$$p_{i,j} = \begin{cases} F_{|h_{\text{SR}}|^2}\left(\dfrac{(j-i+1)C_{\text{P}}}{\eta P_{\text{S}} L}\right) - F_{|h_{\text{SR}}|^2}\left(\dfrac{(j-i)C_{\text{P}}}{\eta P_{\text{S}} L}\right), & i<\varphi \\ (1-q_{\text{SD}})\left[F_{|h_{\text{SR}}|^2}\left(\dfrac{(j-i+1)C_{\text{P}}}{\eta P_{\text{S}} L}\right) - F_{|h_{\text{SR}}|^2}\left(\dfrac{(j-i)C_{\text{P}}}{\eta P_{\text{S}} L}\right)\right], & i \geq \varphi \& C_{\text{M}} < \dfrac{(j-i+q_{\text{FS}}^{\text{c}})C_{\text{P}}}{\eta' L} \\ (1-q_{\text{SD}})\left[F_{|h_{\text{SR}}|^2}\left(\dfrac{(j-i+1)C_{\text{P}}}{\eta P_{\text{S}} L}\right) - F_{|h_{\text{SR}}|^2}\left(\dfrac{(j-i)C_{\text{P}}}{\eta P_{\text{S}} L}\right)\right] & \\ \quad + q_{\text{SD}}\left[1-F_Z\left(\dfrac{(j-i+q_{\text{FS}}^{\text{c}})C_{\text{P}}}{\eta\rho\eta' L}\right)\right], & i \geq \varphi \& \dfrac{(j-i+q_{\text{FS}}^{\text{c}})C_{\text{P}}}{\eta' L} \leq C_{\text{M}} < \dfrac{(j-i+q_{\text{FS}}^{\text{c}}+1)C_{\text{P}}}{\eta' L} \\ (1-q_{\text{SD}})\left[F_{|h_{\text{SR}}|^2}\left(\dfrac{(j-i+1)C_{\text{P}}}{\eta P_{\text{S}} L}\right) - F_{|h_{\text{SR}}|^2}\left(\dfrac{(j-i)C_{\text{P}}}{\eta P_{\text{S}} L}\right)\right] & \\ \quad + q_{\text{SD}}\left[F_Z\left(\dfrac{(j-i+q_{\text{FS}}^{\text{c}}+1)C_{\text{P}}}{\eta\rho\eta' L}\right) - F_Z\left(\dfrac{(j-i+q_{\text{FS}}^{\text{c}})C_{\text{P}}}{\eta\rho\eta' L}\right)\right], & i \geq \varphi \& C_{\text{M}} \geq \dfrac{(j-i+q_{\text{FS}}^{\text{c}}+1)C_{\text{P}}}{\eta' L} \end{cases} \tag{16}$$

$$p_{i,i} = \begin{cases} F_{|h_{\text{SR}}|^2}\left(\dfrac{C_{\text{P}}}{\eta P_{\text{S}} L}\right), & i<\varphi \\ (1-q_{\text{SD}})\,F_{|h_{\text{SR}}|^2}\left(\dfrac{C_{\text{P}}}{\eta P_{\text{S}} L}\right), & i \geq \varphi \& C_{\text{M}} < \dfrac{q_{\text{FS}}^{\text{c}} C_{\text{P}}}{\eta' L} \\ (1-q_{\text{SD}})\,F_{|h_{\text{SR}}|^2}\left(\dfrac{C_{\text{P}}}{\eta P_{\text{S}} L}\right) + q_{\text{SD}}\left[1-F_Z\left(\dfrac{q_{\text{FS}}^{\text{c}} C_{\text{P}}}{\eta\rho\eta' L}\right)\right], & i \geq \varphi \& \dfrac{q_{\text{FS}}^{\text{c}} C_{\text{P}}}{\eta' L} \leq C_{\text{M}} < \dfrac{(q_{\text{FS}}^{\text{c}}+1)C_{\text{P}}}{\eta' L} \\ (1-q_{\text{SD}})\,F_{|h_{\text{SR}}|^2}\left(\dfrac{C_{\text{P}}}{\eta P_{\text{S}} L}\right) + q_{\text{SD}}\left[F_Z\left(\dfrac{(q_{\text{FS}}^{\text{c}}+1)C_{\text{P}}}{\eta\rho\eta' L}\right) - F_Z\left(\dfrac{q_{\text{FS}}^{\text{c}} C_{\text{P}}}{\eta\rho\eta' L}\right)\right], & i \geq \varphi \& C_{\text{M}} \geq \dfrac{(q_{\text{FS}}^{\text{c}}+1)C_{\text{P}}}{\eta' L} \end{cases} \tag{19}$$

be selected and $\Xi_{\text{PEH}} - \Xi_{\text{PEH}}^{\text{C}} \geq E_L - E_i$ should hold. Thus, the transition probability of $E_i \to E_L$ can be expressed as

$$\begin{aligned} p_{i,L} &= \Pr(\gamma_{\text{SD}} \geq \gamma_{th}) \Pr(q_{\text{PEH}} \geq L-i) + \Pr(\gamma_{\text{SD}} < \gamma_{th}) \\ &\quad \times \Pr(E_i < E_{th}) \Pr(q_{\text{PEH}} \geq L-i) + \Pr(\gamma_{\text{SD}} < \gamma_{th}) \\ &\quad \times \Pr(E_i \geq E_{th}) \Pr\left(q_{\text{FS}} - q_{\text{FS}}^{\text{C}} \geq L-i\right) \\ &= \begin{cases} \Pr(q_{\text{PEH}} \geq L-i), & i < \varphi \\ (1-q_{\text{SD}}) \Pr(q_{\text{PEH}} \geq L-i) \\ \quad + q_{\text{SD}} \Pr\left(q_{\text{FS}} - q_{\text{FS}}^{\text{C}} \geq L-i\right), & i \geq \varphi. \end{cases} \end{aligned} \tag{23}$$

Next, $\Pr(q_{\text{PEH}} \geq L-i)$ and $\Pr\left(q_{\text{FS}} - q_{\text{FS}}^{\text{C}} \geq L-i\right)$ can be derived as

$$\begin{aligned} &\Pr(q_{\text{PEH}} \geq L-i) \\ &\quad = 1 - F_{|h_{\text{SR}}|^2}\left[\frac{(L-i)C_{\text{P}}}{\eta P_{\text{S}} L}\right], \end{aligned} \tag{24}$$

$$\begin{aligned} &\Pr\left(q_{\text{FS}} - q_{\text{FS}}^{\text{C}} \geq L-i\right) \\ &\quad = \begin{cases} 0, & C_{\text{M}} < \dfrac{\left(L-i+q_{\text{FS}}^{\text{C}}\right)C_{\text{P}}}{\eta' L} \\ 1 - F_Z\left[\dfrac{\left(L-i+q_{\text{FS}}^{\text{C}}\right)C_{\text{P}}}{\eta\rho\eta' L}\right], & C_{\text{M}} \geq \dfrac{\left(L-i+q_{\text{FS}}^{\text{C}}\right)C_{\text{P}}}{\eta' L}, \end{cases} \end{aligned} \tag{25}$$

respectively.

Invoking (23), (24) and (25), we get the transition probability of $E_i \to E_L$ as (26), shown at the bottom of the next page.

C. Stationary Distribution

Theorem 1: In this theorem, we derive the probability that the energy status of arbitrary transmission slot meets the given energy condition, in a long-term perspective. With the help of stationary distribution $\boldsymbol{\xi}$, for arbitrary transmission slot, we have $\Pr(E_i \geq E_{th}) = \sum_{i=\varphi}^{L} \xi_i$, where φ can be found in (13) and $\xi_i \in \boldsymbol{\xi} = (\xi_0, \xi_1, \ldots, \xi_L)^T$ is defined in the following proof. Furthermore, we can conclude that $\Pr(E_i < E_{th}) = 1 - \sum_{i=\varphi}^{L} \xi_i = \sum_{i=0}^{\varphi-1} \xi_i$.

Proof: We define $\mathbf{M} \triangleq \{p_{i,j}\}$ to denote the $(L+1) \times (L+1)$ state transition matrix. Using the similar methods in [19] and [20], we can easily verify that the transition matrix $\mathbf{M}$ is irreducible[6] and row stochastic.[7] Thus, the stationary distribution $\boldsymbol{\xi}$ must satisfy $\boldsymbol{\xi} = (\xi_0, \xi_1, \ldots, \xi_L)^T = \mathbf{M}^T\boldsymbol{\xi}$. Solving the above equation, $\boldsymbol{\xi}$ can be derived as $\boldsymbol{\xi} = \left(\mathbf{M}^T - \mathbf{I} + \mathbf{B}\right)^{-1} \boldsymbol{b}$ where $\mathbf{B}_{i,j} = 1, \forall i, j$, $\boldsymbol{b} = (1, 1, \ldots, 1)^T$ and $\mathbf{I}$ is the unit matrix. ■

Remark 1: In ***Theorem 1***, ξ_i where $i \in \{0, 1, \ldots, L\}$ represents the stationary probability of the i-th energy state, in a long-term perspective. The reason why the result $\Pr(E_i \geq E_{th}) = \sum_{i=\varphi}^{L} \xi_i$ in ***Theorem 1*** holds can be straight explained as follows: ξ_i $(i \geq \varphi)$ describes the probability of an arbitrary event whose residual energy is higher than the energy threshold and the probability summation of all these events makes up the overall probability of $E_i \geq E_{th}$.

D. Verification and Discussion

In Fig. 1, we illustrate the dynamic charge-discharge behavior of the PEC (subfigure (I)) and the comparison of the steady state distribution gained from the analytical framework in this section against those generated through Monte Carlo simulation (subfigure (II)). Note that for subfigures (I), (II) and (III), $L = 25$; for subfigure (IV), $L = 5$, and other system parameters are all the same among subfigures in Fig. 1. The detailed system parameter setups in this figure is in line with those in Section VI.

Remark 2: The initial energy remained in the PEC is set to be empty, and as the proposed HOR system runs with respect to (w.r.t.) block numbers, the complex energy accumulation and consumption process can be clearly traced as shown in subfigure (I). Observing subfigure (II), it is confirmed that the proposed analytical model matches the actual distribution very well, validating the effectiveness of analysis on the MC in this section.

Remark 3: Comparing subfigures (III) and (IV), one can find that the larger L (i.e., the PEC levels) is, the more likely the residual energy in the PEC can satisfy the "energy requirement" which is hereby quantified as that the residual energy in the PEC is greater than or equal to 60% of the

[6]In a MC, the transition matrix is said to be irreducible if it is possible to reach any other state from any state in finite number of steps. In our MC analysis, all possible energy states communicate so that the transition matrix $\mathbf{M}$ is irreducible.

[7]In a MC, the transition matrix is said to be row stochastic if the sum of all the elements in a row is one and all elements are non-negative. In our MC analysis, the transition probabilities from any energy state to all possible energy states sums up to one and the transition probabilities are definitely non-negative, so we say the transition matrix $\mathbf{M}$ is row stochastic. We also note that $\mathbf{M}$ is asymmetric because $p_{i,j} \neq p_{j,i}$, $\forall i, j$, given the aforementioned analysis.

$$p_{i,j} = \begin{cases} 0, & i < \varphi \| \left(j \geq \varphi \& C_{\text{M}} < \dfrac{\left[q_{\text{FS}}^{\text{C}} - (i-j)\right]C_{\text{P}}}{\eta' L}\right) \\ q_{\text{SD}}\left(1 - F_Z\left(\dfrac{\left[q_{\text{FS}}^{\text{C}} - (i-j)\right]C_{\text{P}}}{\eta\rho\eta' L}\right)\right), & i \geq \varphi \& \dfrac{\left[q_{\text{FS}}^{\text{C}} - (i-j)\right]C_{\text{P}}}{\eta' L} \leq C_{\text{M}} < \dfrac{\left[q_{\text{FS}}^{\text{C}} - (i-j)+1\right]C_{\text{P}}}{\eta' L} \\ q_{\text{SD}}\left[F_Z\left(\dfrac{\left[q_{\text{FS}}^{\text{C}} - (i-j)+1\right]C_{\text{P}}}{\eta\rho\eta' L}\right) - F_Z\left(\dfrac{\left[q_{\text{FS}}^{\text{C}} - (i-j)\right]C_{\text{P}}}{\eta\rho\eta' L}\right)\right], & i \geq \varphi \& C_{\text{M}} \geq \dfrac{\left[q_{\text{FS}}^{\text{C}} - (i-j)+1\right]C_{\text{P}}}{\eta' L} \end{cases} \tag{22}$$

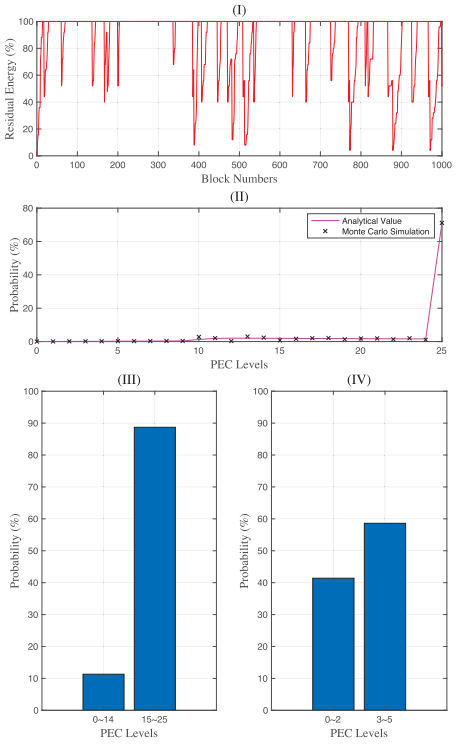

Fig. 1. Illustration of residual energy fluctuations, validation of the proposed MC analysis and the impact of energy discretization levels.

PEC's capacity. This is reasonable for a two-fold reason: 1) the floor function (e.g., formulas (7) and (8)) used to quantify the discretized amount of energy absorbed by the PEC limits that the proposed energy discretization model has to abandon the overflow energy assimilated; 2) the ceil function (e.g., formula (9)) applied to quantify the discretized amount of energy consumed by the PEC restricts that the proposed energy discretization model should quantify the underflow amount of discretized energy used up by the PEC as an specific integer, which means the proposed model consumes extra energy than its actual counterpart. According to the aforementioned analysis, we can conclude that the larger L is, i.e., the finer the PEC is mathematically discretized, the more efficient manipulation of RF energy can be realized. A subsequent influence of L on wireless transmission performance can be found in details in Section VI. However, there exists the inherent trade-off between the computation complexity and energy manipulating efficiency of the proposed energy discretization model so that the value of L should be chosen carefully and delicately in the practical application scenarios.

IV. Covert Communication Performance Analysis

Note that R only intends to broadcast covert message when the FD SWIPT mode is active. Thus, this article focuses on the circumstance in which D performs detection only in the case of the FD SWIPT mode. In the PEH mode, R will not broadcast covert message and D ceases the detection. This consideration is reasonable because the exact work mode R applies is an open consensus among all nodes at the beginning of each specific transmission block. Note that in this section, the constraint $\gamma_{\mathrm{SD}} < \gamma_{th}$ holds due to the nature of the FD SWIPT mode.

A. Channel Uncertainty Model

To investigate the impact of channel uncertainty on covert detection performance at D, it is assumed that D gets an imperfect estimation of the wireless channel R→D and the imperfect channel estimation model of D is formulated as $h_{\mathrm{RD}} = \hat{h}_{\mathrm{RD}} + \tilde{h}_{\mathrm{RD}}$, where $\hat{h}_{\mathrm{RD}} \sim \mathcal{CN}\left(0, (1-\beta)\,\Omega_{\mathrm{RD}}\right)$ and $\tilde{h}_{\mathrm{RD}} \sim \mathcal{CN}\left(0, \beta\Omega_{\mathrm{RD}}\right)$ are independent complex Gaussian random variables (RVs) representing D's channel estimation and the corresponding estimation error, respectively [21]. It is worth noting that $\beta \in (0,1)$ measures the degree of channel uncertainty and the aforementioned Gaussian estimation error comes from the MMSE estimation method.

B. Binary Detection at the Destination

Apart from receiving desired information from S and R, D also needs to perform simple (binary) hypothesis test in which $\mathcal{H}_0$ means the null hypothesis indicating that R does not transmit covert information while $\mathcal{H}_1$ represents the alternative hypothesis implicating that R does emit the covert message. In a specific transmission slot, we define the False Alarm (i.e., type I error) probability by $\mathbb{P}_{\mathrm{FA}} \triangleq \Pr\left(\mathcal{D}_1|\mathcal{H}_0\right)$ and the Missed Detection (i.e., type II error) probability by $\mathbb{P}_{\mathrm{MD}} \triangleq \Pr\left(\mathcal{D}_0|\mathcal{H}_1\right)$, where $\mathcal{D}_1$ and $\mathcal{D}_0$ represent the binary decisions in favor of the occurrence of covert transmission or not, respectively. Besides, *a priori* probabilities of hypotheses $\mathcal{H}_0$ and $\mathcal{H}_1$ are assumed to be equal (i.e., both are 0.5),[8] which is a widely adopted assumption in the field of covert communication. Following this assumption, the detection performance of D is measured by the detection error probability $\mathbb{P}_{\mathrm{E}} \triangleq \mathbb{P}_{\mathrm{FA}} + \mathbb{P}_{\mathrm{MD}}$ [22].

[8]Note that the equal *a priori* probability assumption corresponds to the circumstance in which D has no *a priori* knowledge on whether R emits covert message or not and completely ignores the probability of covert transmissions at R.

$$p_{i,L} = \begin{cases} 1 - F_{|h_{\mathrm{SR}}|^2}\left(\dfrac{(L-i)\,C_{\mathrm{P}}}{\eta P_{\mathrm{S}} L}\right), & i < \varphi \\ (1-q_{\mathrm{SD}})\left[1 - F_{|h_{\mathrm{SR}}|^2}\left(\dfrac{(L-i)\,C_{\mathrm{P}}}{\eta P_{\mathrm{S}} L}\right)\right], & i \geq \varphi \& C_{\mathrm{M}} < \dfrac{\left(L-i+q_{\mathrm{FS}}^{\mathrm{C}}\right)C_{\mathrm{P}}}{\eta' L} \\ (1-q_{\mathrm{SD}})\left[1 - F_{|h_{\mathrm{SR}}|^2}\left(\dfrac{(L-i)\,C_{\mathrm{P}}}{\eta P_{\mathrm{S}} L}\right)\right] + q_{\mathrm{SD}}\left[1 - F_Z\left(\dfrac{\left(L-i+q_{\mathrm{FS}}^{\mathrm{C}}\right)C_{\mathrm{P}}}{\eta\rho\eta' L}\right)\right], & i \geq \varphi \& C_{\mathrm{M}} \geq \dfrac{\left(L-i+q_{\mathrm{FS}}^{\mathrm{C}}\right)C_{\mathrm{P}}}{\eta' L} \end{cases} \tag{26}$$

For arbitrary $\epsilon > 0$, we define that R can achieve covert communication if any communication scheme exists satisfying $\mathbb{P}_{\mathrm{E}} \geq 1-\epsilon$. Note that the lower bound on $\mathbb{P}_{\mathrm{E}}$ characterizes the necessary trade-off between the false alarms and missed detections in a simple hypothesis test. Specifically, $\mathbb{P}_{\mathrm{E}} \geq 1-\epsilon$ represents the covert communication constraint and ϵ signifies the covert requirement, because a sufficiently small ϵ renders any detector employed at D to be ineffective.

C. Derivation and Analysis

In the case of FD SWIPT mode, the received signals at D in the ω-th channel use within a transmission block can be expressed as

$$\boldsymbol{y}_{\mathrm{D}}[\omega] = \begin{cases} \sqrt{P_{\mathrm{S}}} h_{\mathrm{SD}} \boldsymbol{x}_{\mathrm{S}}[\omega] + \sqrt{P_{\mathrm{R}}} h_{\mathrm{RD}} \boldsymbol{x}_{\mathrm{R}}[\omega] + \boldsymbol{n}_{\mathrm{D}}[\omega], & \mathcal{H}_0 \\ \sqrt{P_{\mathrm{S}}} h_{\mathrm{SD}} \boldsymbol{x}_{\mathrm{S}}[\omega] + \sqrt{P_{\mathrm{R}}} h_{\mathrm{RD}} \boldsymbol{x}_{\mathrm{R}}[\omega] \\ \quad + \sqrt{P_{\Delta}} h_{\mathrm{RD}} \boldsymbol{x}_{\mathrm{c}}[\omega] + \boldsymbol{n}_{\mathrm{D}}[\omega], & \mathcal{H}_1. \end{cases} \tag{27}$$

Lemma 1: In the case of availability of noise power at D, it is approved that radiometer is the optimal detector for covert communication detection.

Proof: See Appendix A. ∎

Theorem 2: For arbitrary detection threshold τ of the radiometer, closed-form expressions of false alarm and missed detection probabilities can be given by

$$\mathbb{P}_{\mathrm{FA}} = \begin{cases} \exp\left(\dfrac{j_0 - \tau}{\beta P_{\mathrm{R}} \Omega_{\mathrm{RD}}}\right), & \tau \geq j_0 \\ 1, & \text{otherwise}, \end{cases} \tag{28}$$

$$\mathbb{P}_{\mathrm{MD}} = \begin{cases} 1 - \exp\left[\dfrac{j_1 - \tau}{\beta\left(P_{\mathrm{R}} + P_{\Delta}\right)\Omega_{\mathrm{RD}}}\right], & \tau \geq j_1 \\ 0, & \text{otherwise}, \end{cases} \tag{29}$$

respectively, where $j_0 = P_{\mathrm{S}}|h_{\mathrm{SD}}|^2 + P_{\mathrm{R}}|\hat{h}_{\mathrm{RD}}|^2 + \sigma_{\mathrm{D}}^2$ and $j_1 = P_{\mathrm{S}}|h_{\mathrm{SD}}|^2 + (P_{\mathrm{R}} + P_{\Delta})|\hat{h}_{\mathrm{RD}}|^2 + \sigma_{\mathrm{D}}^2$. Furthermore, invoking (28) and (29), we can derive closed-form expression of $\mathbb{P}_{\mathrm{E}}$ as

$$\mathbb{P}_{\mathrm{E}} = \begin{cases} 1, & \tau < j_0 \\ \exp\left(\dfrac{j_0 - \tau}{\beta P_{\mathrm{R}} \Omega_{\mathrm{RD}}}\right), & j_0 \leq \tau < j_1 \\ 1 + \exp\left(\dfrac{j_0 - \tau}{\beta P_{\mathrm{R}} \Omega_{\mathrm{RD}}}\right) \\ \quad - \exp\left[\dfrac{j_1 - \tau}{\beta\left(P_{\mathrm{R}} + P_{\Delta}\right)\Omega_{\mathrm{RD}}}\right], & \tau \geq j_1. \end{cases} \tag{30}$$

Proof: See Appendix B. ∎

Theorem 3: The optimal detection threshold of D's radiometer, which is supposed to minimize $\mathbb{P}_{\mathrm{E}}$, is given by

$$\tau^* = \begin{cases} j_1, & j_1 \geq \tau_{k_1=0} \\ \tau_{k_1=0}, & j_1 < \tau_{k_1=0}, \end{cases} \tag{31}$$

where

$$\tau_{k_1=0} = -\frac{\beta P_{\mathrm{R}}(P_{\mathrm{R}} + P_{\Delta})\Omega_{\mathrm{RD}}}{P_{\Delta}} \ln \frac{P_{\mathrm{R}}}{P_{\mathrm{R}} + P_{\Delta}} + P_{\mathrm{S}}|h_{\mathrm{SD}}|^2 + \sigma_{\mathrm{D}}^2. \tag{32}$$

Proof: See Appendix C. ∎

Corollary 1: To achieve the best detection performance, D will always select the optimal detection threshold as per (31). Thus, closed-form expression of minimum detection error probability can be calculated as

$$\mathbb{P}_{\mathrm{E}}^* = \begin{cases} \exp\left(\dfrac{j_0 - j_1}{\beta P_{\mathrm{R}} \Omega_{\mathrm{RD}}}\right), & j_1 \geq \tau_{k_1=0} \\ 1 + \exp\left(\dfrac{j_0 - \tau_{k_1=0}}{\beta P_{\mathrm{R}} \Omega_{\mathrm{RD}}}\right) \\ \quad - \exp\left[\dfrac{j_1 - \tau_{k_1=0}}{\beta\left(P_{\mathrm{R}} + P_{\Delta}\right)\Omega_{\mathrm{RD}}}\right], & j_1 < \tau_{k_1=0}. \end{cases} \tag{33}$$

Remark 4: According to ***Theorem 2***, ***Theorem 3*** and ***Corollary 1***, it is confirmed that $\mathbb{P}_{\mathrm{E}}$, τ^* and $\mathbb{P}_{\mathrm{E}}^*$ are independent to parameters k, L, γ_{th}, C_{M}, η, η', σ_{R}^2, h_{RR} and h_{SR}. This is because, concisely speaking, covert communication is constrained to be possible only within the FD SWIPT mode, and parameters C_{P} and E_{th} can affect covert metrics in the manner of the predefined $P_{\mathrm{R}} = E_{th} = 0.6C_{\mathrm{P}}$. Moreover, $\mathbb{P}_{\mathrm{E}}^*$ is not subject to P_{S} and h_{SD} either, because of the subtractions $j_0 - j_1$, $j_0 - \tau_{k1=0}$ and $j_1 - \tau_{k1=0}$. This finding guides designers to understand what parameters are valid to pose impacts on covert communication detection performance.

Corollary 2: Minimum detection error probability $\mathbb{P}_{\mathrm{E}}^*$ monotonically increases w.r.t. β.

Proof: See Appendix D. ∎

Remark 5: Based on ***Corollary 2***, the imperfect channel estimation is proved to be an important factor posing significant impacts on $\mathbb{P}_{\mathrm{E}}^*$. A smaller β, i.e., a better channel estimation method, is desired to enhance the covert communication detection performance at D.

To better show the covert communication performance analysis and verify the correctness of the corresponding analytical expressions, Fig. 2 is illustrated, in which $\beta = 0.5$ holds unless otherwise specified and other system parameters are set in line with those in Section VI. In Fig. 2, we evaluate covert metrics for arbitrarily selected transmission block in which $h_{\mathrm{SD}} = -0.0010 - 0.0027j$ and $h_{\mathrm{RD}} = 0.0261 + 0.0526j$ hold. From subfigure (I), the Monte Carlo simulation nodes match perfectly with the analytical curve of (30) and the dash line generated from (31) coincides tightly with the simulated optimal τ's coordinate, validating the correctness of ***Theorem 2*** and ***Theorem 3***. Subfigure (II) depicts that applying ***Corollary 1*** can significantly reduce the detection error probability, compared with its counterpart without the optimal detection threshold. It can also be observed from subfigure (II) that the curve of $\mathbb{P}_{\mathrm{E}}^*$ keeps a constant w.r.t. P_{S}, the reason can be found in ***Remark 4***. Finally, subfigure (III) shows that $\mathbb{P}_{\mathrm{E}}^*$ monotonically increases w.r.t. β, justifying the effectiveness of ***Corollary 2*** and ***Remark 5***.

V. Transmission Outage Performance Analysis

In this section, transmission outage probability (TOP) is derived and analyzed in details, we consider the circumstance in which D applies Maximum Ratio Combination (MRC) protocol to combine the received signals from S and R, when the FD SWIPT mode is active.

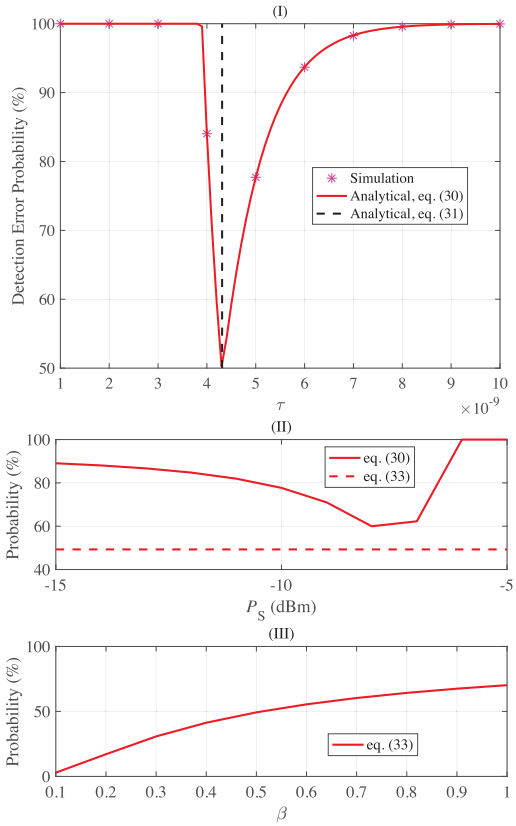

Fig. 2. Validation of the derived closed-form expressions of detection error probability and the optimal detection threshold, illustration of performance superiority of the proposed minimum detection error probability and its monotonicity w.r.t. β.

In the FD SWIPT mode, invoking (3) and (5), the received SINR at D can be given by

$$\gamma_{\rm D} = \begin{cases} \gamma_{\rm SD} + Y_{\mathcal{H}_0}, & \mathcal{H}_0 \\ \gamma_{\rm SD} + Y_{\mathcal{H}_1}, & \mathcal{H}_1, \end{cases} \tag{34}$$

where

$$Y_{\mathcal{H}_0} = \min\left\{\frac{(1-\rho)\,P_{\rm S}|h_{\rm SR}|^2}{(1-\rho)\,kP_{\rm R}|h_{\rm RR}|^2+\sigma_{\rm R}^2}, \frac{P_{\rm R}|h_{\rm RD}|^2}{\sigma_{\rm D}^2}\right\}, \tag{35}$$

$$Y_{\mathcal{H}_1} = \min\left\{\frac{P_{\rm R}|h_{\rm RD}|^2}{P_\Delta|h_{\rm RD}|^2+\sigma_{\rm D}^2}, \frac{(1-\rho)P_{\rm S}|h_{\rm SR}|^2}{(1-\rho)k(P_{\rm R}+P_\Delta)|h_{\rm RR}|^2+\sigma_{\rm R}^2}\right\}. \tag{36}$$

Note that the term $\min\{\cdot,\cdot\}$ in (35) and (36) is introduced by the fixed decode-and-forward (DF) relaying policy applied at R [23], [24]. Knowing $|h_{\rm SR}|^2 \sim E(\Omega_{\rm SR})$, $|h_{\rm RR}|^2 \sim E(\Omega_{\rm RR})$ and $|h_{\rm RD}|^2 \sim E(\Omega_{\rm RD})$, the closed-form CDF expressions of $Y_{\mathcal{H}_0}$ and $Y_{\mathcal{H}_1}$ can be calculated as (37), shown at the bottom of the next page.

Lemma 2: The closed-form expression of CDF of $\gamma_{\rm D}|\mathcal{H}_0$ can be derived as (38) which is shown at the bottom of the next page, where $\mathrm{Ei}(\cdot)$ represents the one-argument exponential integral function. For concise expression, we define the following variables in (38) as $v_1 = \sigma_{\rm D}^2\Omega_{\rm SR}/(kP_{\rm R}\Omega_{\rm RR}\Omega_{\rm SD})$, $v_2 = (\frac{\sigma_{\rm D}^2}{P_{\rm S}\Omega_{\rm SD}} - \frac{\sigma_{\rm R}^2}{(1-\rho)P_{\rm S}\Omega_{\rm SR}} - \frac{\sigma_{\rm D}^2}{P_{\rm R}\Omega_{\rm RD}})/(kP_{\rm R}\Omega_{\rm RR})$, $v_3 = v_2(P_{\rm S}\Omega_{\rm SR} + kP_{\rm R}\Omega_{\rm RR}x)$ and $v_4 = v_2\left[P_{\rm S}\Omega_{\rm SR} + kP_{\rm R}\Omega_{\rm RR}(x-\gamma_{th})\right]$.

Proof: See Appendix E. ■

Lemma 3: The closed-form CDF expression of $\gamma_{\rm D}|\mathcal{H}_1$ in the case of FD SWIPT mode can be derived approximately as

$$F_{\gamma_{\rm D}|\mathcal{H}_1}(x) \approx \mathrm{quadgk}\left(\mathrm{fun}(y), 0, \gamma_{th}\right), \tag{39}$$

where the definitions of $\mathrm{quadgk}(\cdot,\cdot,\cdot)$ and $\mathrm{fun}(y)$ can be found in the following proof.

Proof: See Appendix F. ■

Remark 6: In ***Lemma 3***, the approximation of $F_{\gamma_{\rm D}|\mathcal{H}_1}$ is achieved by converting infinite integral to finite summation. The accuracy of this approximation is mainly affected by the amount of nodes used within the finite summation, the more nodes is applied, the more complex the summation is, though the preciser approximation it can achieve.

Theorem 4: The closed-form expression of the TOP in the FD SWIPT mode is given by

$$TOP_{\rm FS} = \frac{1}{2}\sum_{i=\varphi}^{L}\xi_i\left[F_{\gamma_{\rm D}|\mathcal{H}_0}\left(2^{R_{th}}-1\right) + F_{\gamma_{\rm D}|\mathcal{H}_1}\left(2^{R_{th}}-1\right)\right]. \tag{40}$$

Proof: See Appendix G. ■

Theorem 5: The closed-form expression of the TOP in the PEH mode can be given by

$$TOP_{\rm PEH} = q_{\rm SD}\sum_{i=0}^{\varphi-1}\xi_i + F_{\gamma_{\rm SD}|\gamma_{\rm SD}\geq\gamma_{th}}\left(2^{R_{th}}-1\right), \tag{41}$$

where the concept of $F_{\gamma_{\rm SD}|\gamma_{\rm SD}\geq\gamma_{th}}(x)$ can be found in the following proof.

Proof: See Appendix H. ■

Corollary 3: Finally, invoking (40) and (41), the closed-form expression of overall TOP for our proposed HOR model can be derived as (42), shown at the bottom of the next page.

VI. Numerical Results

In this section, applying the analytical expressions derived in the previous contents, numerical results are simulated and the impacts of key parameters on the TOP performance are investigated. Note that, in Section IV, we have illustrated the effectiveness of the derived covert communication analysis for arbitrary transmission block in the FD SWIPT mode. It is fair to say that the proposed HOR system can always achieve minimum detection error probability for any possible FD SWIPT transmission block, via proactively applying ***Theorem 3*** and ***Corollary 1***. For conciseness, we do not depict covert communication performance in this section. Unless otherwise specified, the simulation results are based on the following parameter setups, which is in line with [19] and [25]. The distances among nodes are set as $d_{\rm SD} = 15$ m, $d_{\rm SR} = 8$ m, $d_{\rm RR} = 0.1$ m and $d_{\rm RD} = 8$ m, where it is reasonable to consider that the distance between R's dual antennas is relatively near. We set the average wireless channel gains as $\Omega_{ij} = 1/(1+d_{ij}^{\alpha}), \{i,j\} \in \{\rm S, R, D\}$, where the path loss exponent is predefined as $\alpha = 3$, the AWGN powers $\sigma_{\rm R}^2 = \sigma_{\rm D}^2 = -60$ dBm, the target transmission rate $R_{th} = 1$ bps/Hz, the SNR threshold $\gamma_{th} = 1$, the energy threshold $E_{th} = 0.6C_{\rm P}$, the transmit power of S $P_{\rm S} = -10$ dBm, the PS

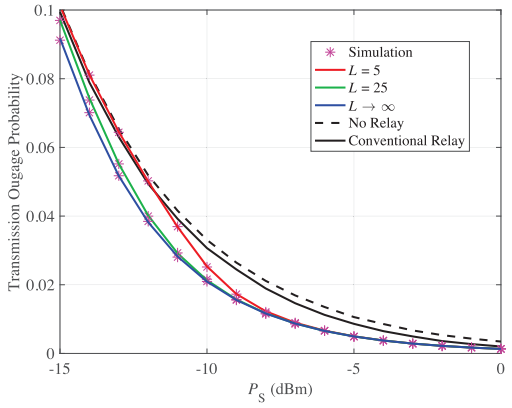

Fig. 3. Transmission outage probability versus P_{S} with various L.

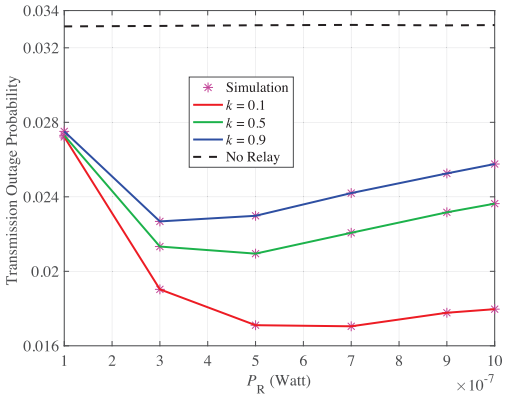

Fig. 4. Transmission outage probability versus P_{R} with various k.

factor $\rho = 0.5$ and the covert transmit power $P_\Delta = 0.2P_{\mathrm{R}}$. Regarding parameters of the hybrid energy storage, we set $C_{\mathrm{P}} = C_{\mathrm{M}} = 10^{-6}$ Joule, $\eta = 0.4$, $\eta' = 0.9$ and $L = 25$.

A. Validation of The Proposed Energy Discretization Method

In this part, we validate the feasibility and accuracy of the proposed discrete energy model described in Section III, by plotting curves generated from the MC-based TOP analysis and the corresponding Monte Carlo simulation points. Note that $L \to \infty$ serves as upper bound of the TOP performance, in the case of a massive energy discretization. For comparison, the conventional relay curve depicts the performance of the most popular FDR scheme in which fixed FD SWIPT relaying mode is applied without energy accumulation. It can be observed from Fig. 3 that even a small energy discretization level ($L = 5$) is enough to provide considerable TOP performance gain for majority of the simulated P_{S} regime, compared to the circumstances in which no relay assists wireless communication or the conventional relay is utilised. Comparing the TOP performance curves of various L values, one can conclude that the TOP performance approaches the upper bound gradually as the value of L increases. The reason why L can affect the HOR system has been explained in details in ***Remark** 3*. Specifically, when L's value is not so large, i.e., $L = 25$, the TOP performance curve can coincide with the upper bound in the most region of simulated P_{S}. The aforementioned observations validate the efficiency and effectiveness of the proposed HOR system on reducing wireless transmission outage, even with practical energy discretization levels ($L = 5, L = 25$).

B. The Impact of R's Transmit Power

In this part, we discuss the impact of P_{R} on the TOP performance. Fig. 4 depicts the TOP curves versus P_{R} with various values of k. It is straightforward to observe that the TOP curves first decrease and then increase with the rising of P_{R}, which turns out that there exists optimal option of P_{R}. The existence of the optimal P_{R} is due to the following two trade-offs: 1) a larger P_{R} will consume more stored energy at the PEC but also lead the PEC to absorb more energy from the SI channel; 2) the min function introduced by the

$$F_{Y_{\mathcal{H}_\phi}}(x) = \begin{cases} 1 - \dfrac{P_{\mathrm{S}}\Omega_{\mathrm{SR}} \exp\left[-\left(\frac{\sigma_{\mathrm{R}}^2}{(1-\rho)P_{\mathrm{S}}\Omega_{\mathrm{SR}}} + \frac{\sigma_{\mathrm{D}}^2}{P_{\mathrm{R}}\Omega_{\mathrm{RD}}}\right)x\right]}{P_{\mathrm{S}}\Omega_{\mathrm{SR}} + kP_{\mathrm{R}}\Omega_{\mathrm{RR}}x}, & \phi = 0 \\ 1 - \dfrac{P_{\mathrm{S}}\Omega_{\mathrm{SR}} \exp\left[-\left(\frac{\sigma_{\mathrm{R}}^2}{(1-\rho)P_{\mathrm{S}}\Omega_{\mathrm{SR}}} + \frac{\sigma_{\mathrm{D}}^2}{(P_{\mathrm{R}}-P_\Delta x)\Omega_{\mathrm{RD}}}\right)x\right]}{P_{\mathrm{S}}\Omega_{\mathrm{SR}} + k\left(P_{\mathrm{R}}+P_\Delta\right)\Omega_{\mathrm{RR}}x}, & \phi = 1 \& x < \dfrac{P_{\mathrm{R}}}{P_\Delta} \\ 1, & \phi = 1 \& x \geq \dfrac{P_{\mathrm{R}}}{P_\Delta} \end{cases} \tag{37}$$

$$F_{\gamma_{\mathrm{D}}|\mathcal{H}_0}(x) = q_{\mathrm{SD}} - v_1\left[\mathrm{Ei}(v_3) - \mathrm{Ei}(v_4)\right] \exp\left[\frac{P_{\mathrm{S}}\Omega_{\mathrm{SR}}\left(\frac{\sigma_{\mathrm{R}}^2}{(1-\rho)P_{\mathrm{S}}\Omega_{\mathrm{SR}}} + \frac{\sigma_{\mathrm{D}}^2}{P_{\mathrm{R}}\Omega_{\mathrm{RD}}}\right) - \frac{\sigma_{\mathrm{D}}^2}{P_{\mathrm{S}}\Omega_{\mathrm{SD}}}\left(P_{\mathrm{S}}\Omega_{\mathrm{SR}} + kP_{\mathrm{R}}\Omega_{\mathrm{RR}}x\right)}{kP_{\mathrm{R}}\Omega_{\mathrm{RR}}}\right] \tag{38}$$

$$TOP = q_{\mathrm{SD}} \sum_{i=0}^{\varphi-1} \xi_i + F_{\gamma_{\mathrm{SD}}|\gamma_{\mathrm{SD}} \geq \gamma_{th}}\left(2^{R_{th}} - 1\right) + \frac{1}{2}\sum_{i=\varphi}^{L} \xi_i \left[F_{\gamma_{\mathrm{D}}|\mathcal{H}_0}\left(2^{R_{th}} - 1\right) + F_{\gamma_{\mathrm{D}}|\mathcal{H}_1}\left(2^{R_{th}} - 1\right)\right] \tag{42}$$

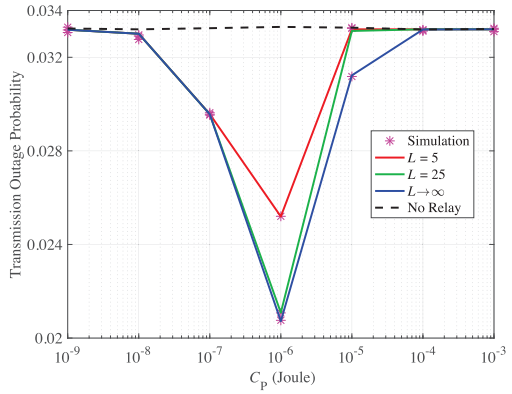

Fig. 5. Transmission outage probability versus C_{P} with various L.

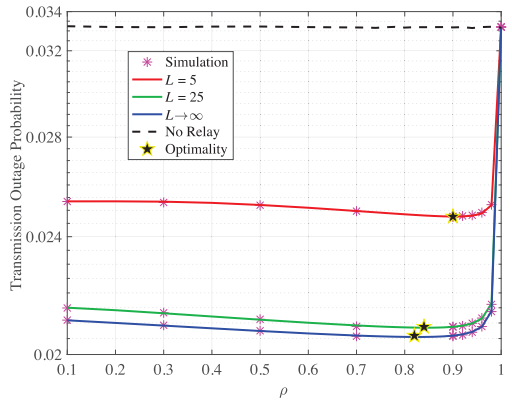

Fig. 6. Transmission outage probability versus ρ with various L.

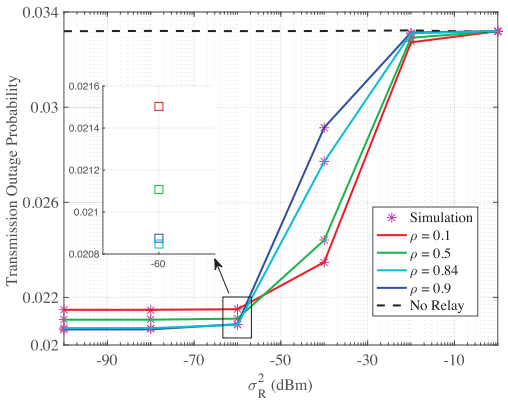

Fig. 7. Transmission outage probability versus σ_{R}^2 with various ρ.

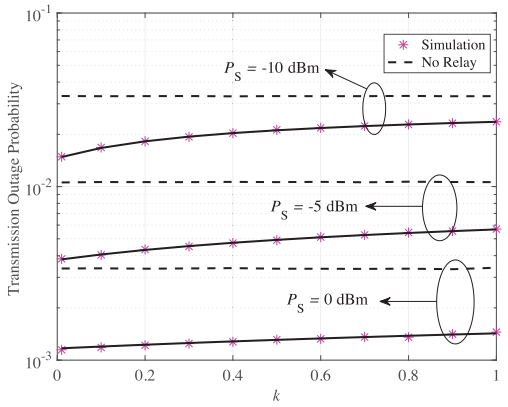

Fig. 8. Transmission outage probability versus k with various P_{S}.

DF relaying strategy limits that γ_{D} is not always increasing with the increase of P_{R}. This two kinds of dilemma cause that simply enlarging P_{R} does not lead to a better TOP performance, and also make the optimal value of P_{R} existing. This finding is beneficial for designer to choose a feasible value of P_{R} in implement of the proposed HOR system.

C. The Impact of Capacity of The PEC

In this subsection, we examine how C_{P} influences the TOP performance. Fig. 5 shows the TOP curves versus C_{P} with various L values. It is straightforward to find that for specific HOR system parameter setup, there exists optimal value of C_{P} to minimize the TOP performance. The existence of the optimal C_{P} is because, briefly speaking, it influences the values of P_{R} and E_{th} by the means of $P_{\mathrm{R}} = E_{th} = 0.6C_{\mathrm{P}}$. Under the system parameter setup of this example, the values of L does not pose any impact on value of the optimal C_{P}. It can be observed that $L = 25$ can almost act as a feasible alternative of the TOP performance's upper bound, revealing the efficiency of the proposed energy discretization model. The observation of this example allows the system designer to determine an optimal C_{P} while reducing computation by selecting a small but sufficient L, for various system parameter setups.

D. The Impact of The PS Factor

In this part, we investigate the impact of ρ on the TOP performance. Fig. 6 demonstrates the TOP curves versus ρ with various L values. Alongside all the possible values of ρ towards $\rho = 1$, we can find that the TOP curves first decreases, reach the optimality and then rocket to the worst case at which performance gain offered by the proposed HOR protocol does not exist any more. The existence of the optimality is because the inherent trade-off at R between harvesting more energy and gaining stronger received SNR. Also, one can find that the energy discretization levels does pose impact on the value of the optimality. Specifically, a larger L leads to a smaller value of the optimality. It does make sense because a larger L can reduce the energy loss in the proposed energy discretization model based on the discussion in ***Remark** 3* so that R has the space to pose more efforts on information processing.

E. The Impact of R's AWGN Power

In this subsection, we show the influence of σ_{R}^2 on the TOP performance. Fig. 7 depicts the TOP curves versus σ_{R}^2 with various values of ρ. From the figure, it is straightforward to conclude that the TOP performance decreases with the increase of σ_{R}^2. Specifically, when R is less or equally "noisy" than D, i.e., in the case of $\sigma_{\mathrm{R}}^2 \leq \sigma_{\mathrm{D}}^2$, the TOP performance remains static at the minimum value. On the contrary, a "noisier" R will lead to the loss of performance gain offered by the proposed HOR system. This is because, in short, the min function introduced by the DF relaying strategy in formulas (35) and (36) forces the overall received SNR γ_{D} to behave the segmentation feature. Besides, with the increase of σ_{R}^2,

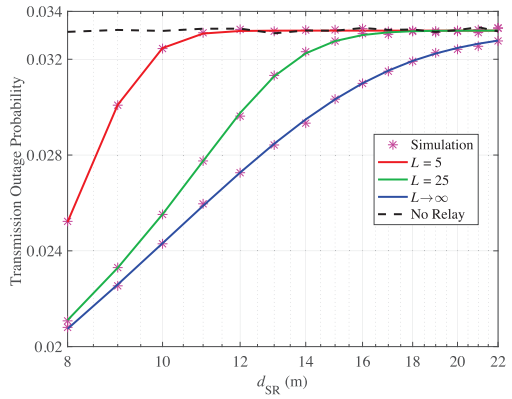

Fig. 9. Transmission outage probability versus d_{SR} with various L.

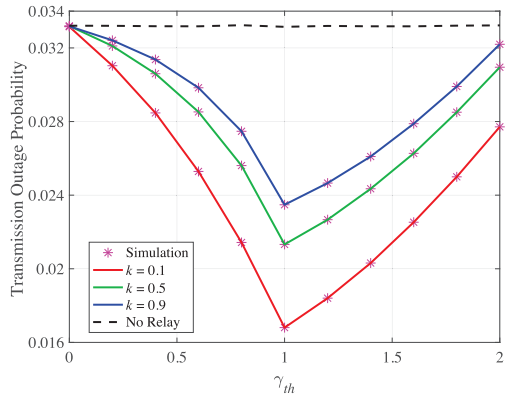

Fig. 10. Transmission outage probability versus γ_{th} with various k.

the impact of ρ on the TOP performance gradually becomes negligible, e.g., in the case of $\rho \in [-20, 0]$ dBm. This is because, at this moment, $Y_{\mathcal{H}_i}, i \in \{0, 1\}$ is way too small compared with γ_{SD}. Moreover, we give the detailed illustration in the case of $\sigma_R^2 = -60$ dBm. At this point, the TOP performance of $\rho = 0.84$ (the empirical optimal PS factor from Fig. 6) is superior to that of $\rho = 0.9$, validating the existence of the optimal ρ discussed in the aforementioned Subsection D.

F. The Impact of SIC Strength

In this part, we examine how k affects the TOP performance. Fig. 8 shows the TOP curves versus k with various P_S values. It is obvious that the TOP performance is becoming worse with the increase of k, for all simulated P_S setups, since a larger k means a stronger SI which suppresses the received SNR of R more. Although a larger k can lead R to harvest more energy from the loop SI channel, from Fig. 8, it is still better to pursue a good SIC efficiency, i.e., a smaller value of k, when implementing the proposed HOR system. Besides, with a higher P_S, the impact of k becomes less obvious. This is because the strengths of both energy harvested from the SI channel and the interference caused by the SI link become minor, in the case of a high value of P_S, which is determined by formulas (6), (35) and (36).

G. The Impact of The Distance Between S and R

In this subsection, we discuss the impact of d_{SR} on the TOP performance. Under the subjective of the Triangle Side Length Rule, the possible length of d_{SR} should locates in $d_{SR} \in (7, 23)$ m. From Fig. 9, it is easy to find that no matter what L's value is, a reasonable shorter distance between S and R is always preferred for achieving more TOP performance gain. The reason is simply because the amount of harvested energy is very sensitive to d_{SR}, which can be found in the assumption of $\Omega_{SR} = 1/(1+d_{SR}^3)$. From this figure, the approaching speed of the TOP curves to the "No Relay" line is much slower for a larger L, validating the discussion in ***Remark** 3*.

H. The Impact of The SNR Threshold

In this part, we analyse how the value of γ_{th} affects the TOP performance. Fig. 10 depicts the TOP curves versus γ_{th} with different k values. From this figure, one can observe that there exists an optimal value of γ_{th} which can minimize the TOP curves. This is because, concisely speaking, the value of γ_{th} directly influences the occurrence frequency of the FD SWIPT mode, which is determined by the activation condition as $\{\gamma_{SD} < \gamma_{th}\} \cap \{E_i \geq E_{th}\}$. The dilemma of "never or less frequently using R" and "using R too much" makes the optimal γ_{th} possible. Besides, the optimal value of γ_{th} is independent to k. However, a more solid SIC degree, i.e., a smaller k, is still preferable, which is consistent with the discussion in Subsection F.

VII. Conclusion

In this article, we initiated a novel wireless relaying transmission scheme termed as HOR. To realise the SWIPT and true FD functionalities, a practical finite-capacity hybrid energy storage model is applied. The relay can work opportunistically in either the PEH or the FD SWIPT mode, not only providing a smarter way to manipulate available wireless energy but also improving the overall wireless transmission performance. To track the dynamic charge-discharge behaviour of the PEC, a discrete-state MC method is adopted, based on which the stationary distribution of energy states is quantified. Furthermore, covert communication and transmission performances of the proposed HOR system were analysed via deriving closed-form expressions of minimum detection error probability and transmission outage probability. Numerical results validated the correctness of the aforementioned analyses and the impacts of key system parameters were discussed. Through analytical derivation and numerical simulation, it is proved that the proposed HOR scheme can enhance wireless energy manipulating efficiency, wireless transmission outage performance and privacy level, which provides a better solution for wireless relaying networks.

Appendix A
Proof of Lemma 1

As each symbol of the received message vector $\boldsymbol{y}_D$ in a specific transmission slot follows i.i.d. complex Gaussian

distribution, $\boldsymbol{y}_{\mathrm{D}}[\omega]$ is ruled by the following distribution

$$\begin{cases}\mathcal{CN}\left(0, P_{\mathrm{S}}|h_{\mathrm{SD}}|^2+P_{\mathrm{R}}|\hat{h}_{\mathrm{RD}}|^2+P_{\mathrm{R}}|\tilde{h}_{\mathrm{RD}}|^2+\sigma_{\mathrm{D}}^2\right), & \mathcal{H}_0\\ \mathcal{CN}\left(0, P_{\mathrm{S}}|h_{\mathrm{SD}}|^2+\left(P_{\mathrm{R}}+P_{\Delta}\right)|\hat{h}_{\mathrm{RD}}|^2\right.\\ \quad\left.+\left(P_{\mathrm{R}}+P_{\Delta}\right)|\tilde{h}_{\mathrm{RD}}|^2+\sigma_{\mathrm{D}}^2\right), & \mathcal{H}_1.\end{cases} \tag{43}$$

Denote the observation conditioned on ψ by $\boldsymbol{y}_{\mathrm{D}}(\psi) = [y_{\mathrm{D}}[1](\psi), y_{\mathrm{D}}[2](\psi), \ldots, y_{\mathrm{D}}[n](\psi)]$ in which $y_{\mathrm{D}}[\omega](\psi) \sim \mathcal{CN}\left(0, \sigma_{\mathrm{D}}^2+\psi\right)$. Note that ψ represents the sum variance of D's received signals from S and R. To distinguish the null hypothesis $\mathcal{H}_0$ from the alternative hypothesis $\mathcal{H}_1$, we here introduce a couple of non-negative and real-value RVs Ψ_0 and Ψ_1, whose PDFs are integratedly given by

$$f_{\Psi_q}(\psi) = \begin{cases}\dfrac{\exp\left(-\frac{\psi-\phi_0}{\beta P_{\mathrm{R}}\Omega_{\mathrm{RD}}}\right)}{\beta P_{\mathrm{R}}\Omega_{\mathrm{RD}}}, & x>\phi_0,\ q=0\\ \dfrac{\exp\left[-\frac{\psi-\phi_1}{\beta\left(P_{\mathrm{R}}+P_{\Delta}\right)\Omega_{\mathrm{RD}}}\right]}{\beta\left(P_{\mathrm{R}}+P_{\Delta}\right)\Omega_{\mathrm{RD}}}, & x>\phi_1,\ q=1\\ 0, & \text{otherwise,}\end{cases} \tag{44}$$

where $\phi_0 = P_{\mathrm{S}}\Omega_{\mathrm{SD}} + (1-\beta)P_{\mathrm{R}}\Omega_{\mathrm{RD}}$ and $\phi_1 = P_{\mathrm{S}}\Omega_{\mathrm{SD}} + (1-\beta)\left(P_{\mathrm{R}}+P_{\Delta}\right)\Omega_{\mathrm{RD}}$.

Furthermore, the PDF of vector $\boldsymbol{y}_{\mathrm{D}}$ given ψ can be calculated as

$$\begin{aligned} f_{\boldsymbol{y}_{\mathrm{D}}(\psi)}(\boldsymbol{y}) &= \prod_{\omega=1}^{n}\frac{\exp\left(-\frac{|\boldsymbol{y}_{\mathrm{D}}[\omega](\psi)|^2}{\sigma_{\mathrm{D}}^2+\psi}\right)}{\pi(\sigma_{\mathrm{D}}^2+\psi)}\\ &= \left[\frac{1}{\pi\left(\sigma_{\mathrm{D}}^2+\psi\right)}\right]^n\exp\left(-\frac{\sum_{\omega=1}^{n}|\boldsymbol{y}_{\mathrm{D}}[\omega](\psi)|^2}{\sigma_{\mathrm{D}}^2+\psi}\right). \end{aligned} \tag{45}$$

Here, invoking the Fisher-Neyman Factorization Theorem [26], the total received power in a transmission slot $\sum_{\omega=1}^{n}|\boldsymbol{y}_{\mathrm{D}}[\omega](\psi)|^2$ is a sufficient statistic for D's hypothesis test. It is worth noting that $\sum_{\omega=1}^{n}|\boldsymbol{y}_{\mathrm{D}}[\omega](\psi)|^2 = \left(\sigma_{\mathrm{D}}^2+\psi\right)\mathcal{X}_{2n}^2$ where $\mathcal{X}_{2n}^2$ denotes chi-squared RV with $2n$ degrees of freedom. Because D knows the statistical knowledge of his received signals when either hypothesis holds, with the help of the Neyman-Pearson Lemma, the best testing rule for D to decide which hypothesis holds is the likelihood ratio test (LRT), given by

$$\Lambda(\boldsymbol{y}_{\mathrm{D}}) = \frac{f_{\boldsymbol{y}_{\mathrm{D}}|\mathcal{H}_1}(\boldsymbol{y})}{f_{\boldsymbol{y}_{\mathrm{D}}|\mathcal{H}_0}(\boldsymbol{y})} \underset{\mathcal{D}_0}{\overset{\mathcal{D}_1}{\gtrless}} \Gamma, \tag{46}$$

where $\Gamma = \Pr(\mathcal{H}_1)/\Pr(\mathcal{H}_0) = 1$ due to the application of equal *a priori* assumption. D does not have instantaneous knowledge of either Ψ_0 or Ψ_1, so he modifies his LRT as

$$\Lambda(\boldsymbol{y}_{\mathrm{D}}) = \frac{\mathbb{E}_{\Psi_1}\left[f_{\boldsymbol{y}_{\mathrm{D}}(\psi)}(\boldsymbol{y})\right]}{\mathbb{E}_{\Psi_0}\left[f_{\boldsymbol{y}_{\mathrm{D}}(\psi)}(\boldsymbol{y})\right]} \underset{\mathcal{D}_0}{\overset{\mathcal{D}_1}{\gtrless}} \Gamma. \tag{47}$$

We introduce here that RV X is smaller than RV Y in the likelihood ratio order, i.e., $X \leq_{\mathrm{lr}} Y$, when $f_Y(x)/f_X(x)$ is a non-decreasing function over the union of their supports.

Invoking (44), we have

$$\frac{f_{\Psi_1}(\psi)}{f_{\Psi_0}(\psi)} = \frac{P_{\mathrm{R}}}{P_{\mathrm{R}}+P_{\Delta}}\exp\left[\frac{P_{\Delta}\psi-\left(P_{\mathrm{R}}+P_{\Delta}\right)\phi_0+P_{\mathrm{R}}\phi_1}{\beta P_{\mathrm{R}}\left(P_{\mathrm{R}}+P_{\Delta}\right)\Omega_{\mathrm{RD}}}\right]. \tag{48}$$

It is straightforward to find that (48) is non-decreasing over the union of supports of Ψ_0 and Ψ_1, hence $\Psi_0 \leq_{\mathrm{lr}} \Psi_1$. From the statistical nature of chi-squared RVs, for any $\psi_1 \leq \psi_2$, we have $\boldsymbol{y}_{\mathrm{D}}(\psi_1) \leq_{\mathrm{lr}} \boldsymbol{y}_{\mathrm{D}}(\psi_2)$. Then, according to Theorem 1, Chapter 11 in [27], the monotonicity of $\Lambda(\boldsymbol{y}_{\mathrm{D}})$ is ruled by Stochastic Ordering and $\Lambda(\boldsymbol{y}_{\mathrm{D}})$ is non-decreasing w.r.t. $\sum_{\omega=1}^{n}|\boldsymbol{y}_{\mathrm{D}}[\omega](\psi)|^2$. Hence, the LRT (47) is equivalent to a received power threshold test. Since any one-to-one transformation of a sufficient statistic remains the sufficiency, the term $\sum_{\omega=1}^{n}|\boldsymbol{y}_{\mathrm{D}}[\omega]|^2/n$ is also a sufficient statistic. Invoking the Lebesgue's Dominated Convergence Theorem, it is allowed to replace $\mathcal{X}_{2n}^2/n$ by 1 when $n\to\infty$. Thus, we get

$$\begin{aligned} T &= \lim_{n\to\infty}\frac{1}{n}\sum_{\omega=1}^{n}|\boldsymbol{y}_{\mathrm{D}}[\omega]|^2\\ &= \begin{cases}P_{\mathrm{S}}|h_{\mathrm{SD}}|^2+P_{\mathrm{R}}|\hat{h}_{\mathrm{RD}}|^2+P_{\mathrm{R}}|\tilde{h}_{\mathrm{RD}}|^2+\sigma_{\mathrm{D}}^2, & \mathcal{H}_0\\ P_{\mathrm{S}}|h_{\mathrm{SD}}|^2+\left(P_{\mathrm{R}}+P_{\Delta}\right)|\hat{h}_{\mathrm{RD}}|^2\\ \quad+\left(P_{\mathrm{R}}+P_{\Delta}\right)|\tilde{h}_{\mathrm{RD}}|^2+\sigma_{\mathrm{D}}^2, & \mathcal{H}_1.\end{cases} \end{aligned} \tag{49}$$

Then, the optimal decision rule at D can be expressed as $T \underset{\mathcal{D}_0}{\overset{\mathcal{D}_1}{\gtrless}} \tau$ where τ denotes the threshold which will be optimized to minimize $\mathbb{P}_{\mathrm{E}}$. After all, a radiometer which is able to detect the total power of received messages at D is proved to be optimal.

Appendix B
Proof of Theorem 2

Invoking (49), we can calculate the false alarm and missed detection probabilities as

$$\begin{aligned} \mathbb{P}_{\mathrm{FA}} &= \Pr(T>\tau|\mathcal{H}_0) = \Pr\left(P_{\mathrm{R}}|\tilde{h}_{\mathrm{RD}}|^2+j_0>\tau\right)\\ &= \begin{cases}\Pr\left(|\tilde{h}_{\mathrm{RD}}|^2>\dfrac{\tau-j_0}{P_{\mathrm{R}}}\right), & \tau\geq j_0\\ 1, & \text{otherwise,}\end{cases} \end{aligned} \tag{50}$$

$$\begin{aligned} \mathbb{P}_{\mathrm{MD}} &= \Pr(T<\tau|\mathcal{H}_1) = \Pr\left[\left(P_{\mathrm{R}}+P_{\Delta}\right)|\tilde{h}_{\mathrm{RD}}|^2+j_1<\tau\right]\\ &= \begin{cases}\Pr\left(|\tilde{h}_{\mathrm{RD}}|^2<\dfrac{\tau-j_1}{P_{\mathrm{R}}+P_{\Delta}}\right), & \tau\geq j_1\\ 0, & \text{otherwise.}\end{cases} \end{aligned} \tag{51}$$

Because the uncertain part of channel R→D follows the distribution $\tilde{h}_{\mathrm{RD}} \sim \mathcal{CN}(0, \beta\Omega_{\mathrm{RD}})$, it is straightforward to know that $|\tilde{h}_{\mathrm{RD}}|^2$ obeys the exponential distribution. Thus, the CDF of $|\tilde{h}_{\mathrm{RD}}|^2$ can be gained as $F_{|\tilde{h}_{\mathrm{RD}}|^2}(x) = 1-\exp\left[-x/(\beta\Omega_{\mathrm{RD}})\right]$. Then, after some simple algebra calculations, we gain the closed-form expressions of false alarm and missed detection probabilities as (28) and (29), respectively. Invoking (28) and (29), closed-form expression of detection error probability can be gained after simple derivation as (30).

Appendix C
Proof of Theorem 3

To determine the optimal detection threshold of D's radiometer, it is supposed to solve the optimization problem as $\tau^* = \arg\min_{\tau}\mathbb{P}_{\mathrm{E}}$. In the case of $\tau < j_0$, the detection error probability at D remains 1. This is the worst case for D and

D will never choose any value satisfying $\tau < j_0$. In the case of $j_0 \leq \tau < j_1$, it is easy to find that $\mathbb{P}_{\mathrm{E}}$ monotonically decreases w.r.t. τ. Besides, the piecewise function $\mathbb{P}_{\mathrm{E}}$ is a continuous function alongside the whole feasible domain of τ. Thus, D will choose j_1 to minimize $\mathbb{P}_{\mathrm{E}}$, leading to $\mathbb{P}_{\mathrm{E}} = \exp\left[\left(j_0 - j_1\right) / \left(\beta P_{\mathrm{R}} \Omega_{\mathrm{RD}}\right)\right]$.

In the case of $\tau \geq j_1$, to determine the optimal value of τ, the first derivative of function $\mathbb{P}_{\mathrm{E}}$ w.r.t. τ is calculated as

$$\frac{\partial \mathbb{P}_{\mathrm{E}}}{\partial \tau} = \frac{k}{\beta P_{\mathrm{R}} \left(P_{\mathrm{R}} + P_{\Delta}\right) \Omega_{\mathrm{RD}}}, \tag{52}$$

where $k = P_{\mathrm{R}} \exp\left[\left(j_1 - \tau\right) / \left(\beta \left(P_{\mathrm{R}} + P_{\Delta}\right) \Omega_{\mathrm{RD}}\right)\right] - \left(P_{\mathrm{R}} + P_{\Delta}\right) \exp\left[\left(j_0 - \tau\right) / \left(\beta P_{\mathrm{R}} \Omega_{\mathrm{RD}}\right)\right]$. It is easy to find that whether (52) is positive or not depends only on the value of k. After simple manipulations, we can modify k as

$$k = \exp\left[\ln P_{\mathrm{R}} + \frac{j_1 - \tau}{\beta \left(P_{\mathrm{R}} + P_{\Delta}\right) \Omega_{\mathrm{RD}}}\right] - \exp\left[\ln\left(P_{\mathrm{R}} + P_{\Delta}\right) + \frac{j_0 - \tau}{\beta P_{\mathrm{R}} \Omega_{\mathrm{RD}}}\right]. \tag{53}$$

Besides, the exponential function exp is monotonically increasing w.r.t. the feasible independent variable region. Thus, we can determine whether k is positive or not by

$$\begin{aligned} k_1 &= \ln \frac{P_{\mathrm{R}}}{P_{\mathrm{R}} + P_{\Delta}} + \frac{P_{\mathrm{R}} \left(j_1 - \tau\right) - \left(P_{\mathrm{R}} + P_{\Delta}\right)\left(j_0 - \tau\right)}{\beta P_{\mathrm{R}} \left(P_{\mathrm{R}} + P_{\Delta}\right) \Omega_{\mathrm{RD}}} \\ &= \ln \frac{P_{\mathrm{R}}}{P_{\mathrm{R}} + P_{\Delta}} + \frac{P_{\Delta}\left(\tau - P_{\mathrm{S}} |h_{\mathrm{SD}}|^2 - \sigma_{\mathrm{D}}^2\right)}{\beta P_{\mathrm{R}} \left(P_{\mathrm{R}} + P_{\Delta}\right) \Omega_{\mathrm{RD}}}. \end{aligned} \tag{54}$$

Because $\tau \geq j_1$ stands in this considered case, the right hand of (54) is absolutely positive. However, the left hand of (54) is negative due to $P_{\mathrm{R}} < P_{\mathrm{R}} + P_{\Delta}$. Most importantly, from (54), we can find that k_1 is a monotonically increasing function w.r.t. τ. Let $k_1 = 0$, we can get the solution as (32). From (32), we can conclude that $k_1 \geq 0$ in the case of $\tau \geq \tau_{k_1=0}$ and $k_1 < 0$ otherwise. If $j_1 \geq \tau_{k_1=0}$ holds, in the case of $\tau \geq j_1$, we can determine that $k > 0$ and furthermore $\partial \mathbb{P}_{\mathrm{E}} / \partial \tau > 0$ which means $\mathbb{P}_{\mathrm{E}}$ monotonically increases w.r.t. τ when $\tau \geq j_1$. Here, it is the optimal choice for D to choose j_1 as the optimal threshold which is able to minimize $\mathbb{P}_{\mathrm{E}}$. If $j_1 < \tau_{k_1=0}$, we know that for $\tau \in (j_1, \tau_{k_1=0})$, $\partial \mathbb{P}_{\mathrm{E}} / \partial \tau < 0$ and for $\tau \in (\tau_{k_1=0}, +\infty)$, $\partial \mathbb{P}_{\mathrm{E}} / \partial \tau > 0$. Thus, the optimal detection threshold for D is $\tau_{k_1=0}$ in this case.

Appendix D
Proof of Corollary 2

In the case of $j_1 \geq \tau_{k_1=0}$, i.e., $\beta \geq -P_{\Delta} |\hat{h}_{\mathrm{RD}}|^2 / \left(P_{\mathrm{R}} \Omega_{\mathrm{RD}} \ln \frac{P_{\mathrm{R}}}{P_{\mathrm{R}} + P_{\Delta}}\right)$, the first derivative of $\mathbb{P}_{\mathrm{E}}^*$ w.r.t. β can be calculated as

$$\frac{\partial \mathbb{P}_{\mathrm{E}}^*}{\partial \beta} \mid_{j_1 \geq \tau_{k_1=0}} = -\frac{j_0 - j_1}{\beta^2 P_{\mathrm{R}} \Omega_{\mathrm{RD}}} \exp\left(\frac{j_0 - j_1}{\beta P_{\mathrm{R}} \Omega_{\mathrm{RD}}}\right), \tag{55}$$

whose value is positive due to $j_0 < j_1$. For $j_1 < \tau_{k_1=0}$, i.e., $\beta < -P_{\Delta} |\hat{h}_{\mathrm{RD}}|^2 / \left(P_{\mathrm{R}} \Omega_{\mathrm{RD}} \ln \frac{P_{\mathrm{R}}}{P_{\mathrm{R}} + P_{\Delta}}\right)$, the first derivative of $\mathbb{P}_{\mathrm{E}}^*$ w.r.t. β can be calculated as

$$\begin{aligned} \frac{\partial \mathbb{P}_{\mathrm{E}}^*}{\partial \beta} \mid_{j_1 < \tau_{k_1=0}} &= \frac{|\hat{h}_{\mathrm{RD}}|^2}{\beta^2 \Omega_{\mathrm{RD}}} \left[\exp\left(\frac{|\hat{h}_{\mathrm{RD}}|^2}{\beta^2 \Omega_{\mathrm{RD}}} + \frac{P_{\mathrm{R}}}{P_{\Delta}} \ln \frac{P_{\mathrm{R}}}{P_{\mathrm{R}} + P_{\Delta}}\right)\right. \\ &\quad \left. - \exp\left(\frac{|\hat{h}_{\mathrm{RD}}|^2}{\beta^2 \Omega_{\mathrm{RD}}} + \frac{P_{\mathrm{R}} + P_{\Delta}}{P_{\Delta}} \ln \frac{P_{\mathrm{R}}}{P_{\mathrm{R}} + P_{\Delta}}\right)\right], \end{aligned} \tag{56}$$

whose value is also positive due to the truth of $P_{\mathrm{R}} > P_{\Delta} > 0$. Thus, we can conclude that $\mathbb{P}_{\mathrm{E}}^*$ monotonically increases as β increases.

Appendix E
Proof of Lemma 2

The CDF of $\gamma_{\mathrm{D}} | \mathcal{H}_0$ can be constructed as $F_{\gamma_{\mathrm{D}} | \mathcal{H}_0}(x) = \Pr\left(\gamma_{\mathrm{SD}} + Y_{\mathcal{H}_0} < x \bigcap \gamma_{\mathrm{SD}} < \gamma_{th}\right)$. Note that the limitation of variable γ_{SD} should be constrained as $\gamma_{\mathrm{SD}} < \gamma_{th}$ due to the nature of FD SWIPT mode. Invoking (37) and after some simple mathematical computations, we can obtain the closed-form expression of $F_{\gamma_{\mathrm{D}} | \mathcal{H}_0}(x)$ as (38).

Appendix F
Proof of Lemma 3

The closed-form CDF expression of $\gamma_{\mathrm{D}} | \mathcal{H}_1$ should be calculated in the way similar to the derivation of (38). However, we found that it is mathematically intractable. To tackle this problem, we resort to the Gauss-Kronrod Quadrature (GKQ) method to approximately solve it, shown as

$$\begin{aligned} F_{\gamma_{\mathrm{D}} | \mathcal{H}_1}(x) &= \Pr\left[\gamma_{\mathrm{SD}} + Y_{\mathcal{H}_1} < x \bigcap \gamma_{\mathrm{SD}} < \gamma_{th}\right] \\ &= \int_0^{\gamma_{th}} \underbrace{\frac{\sigma_{\mathrm{D}}^2}{P_{\mathrm{S}} \Omega_{\mathrm{SD}}} F_{Y_{\mathcal{H}_1}}(x - y) \exp\left(-\frac{\sigma_{\mathrm{D}}^2 y}{P_{\mathrm{S}} \Omega_{\mathrm{SD}}}\right)}_{\mathrm{fun}} dy \\ &\approx \sum_{i=1}^{n} \varrho_i \mathrm{fun}\left(y_i\right), \end{aligned} \tag{57}$$

where ϱ_i and y_i denote the weights and points which are essential to evaluate the function $\mathrm{fun}(y)$. Note that the GKQ formula is an adaptive method for numerical integration, which is a variant of Gaussian quadrature. We use the built-in function of Matlab named $\mathrm{quadgk}(\cdot, \cdot, \cdot)$ to calculate (57), which employs adaptive quadrature based on a Gauss-Kronrod pair (15^{th} and 7^{th} order formulas). Thus, we can derive the closed-form approximate CDF expression of $\gamma_{\mathrm{D}} | \mathcal{H}_1$ as (39).

Appendix G
Proof of Theorem 4

In our considered HOR model, the TOP in the case of FD SWIPT should be constructed as (58) which is shown at the top of the next page, where the factor $1/2$ is due to the assumption of equal *a priori*, R_{th} is the target rate under which the transmission outage occurs. Note that step (a) in (58) holds, because of the fact that the energy requirement is independent of other factors. With the help of ***Lemma 2*** and ***Lemma 3***, we are able to derive the closed-form expressions of f_1 and

$$
\begin{aligned}
TOP_{\mathrm{FS}} &= \Pr\left[\log_2\left(1+\gamma_{\mathrm{D}}\right) < R_{th} \bigcap \mathcal{H}_0 \bigcap \mathrm{FS}\right] + \Pr\left[\log_2\left(1+\gamma_{\mathrm{D}}\right) < R_{th} \bigcap \mathcal{H}_1 \bigcap \mathrm{FS}\right] \\
&\overset{a}{=} \Pr\left[\log_2\left(1+\gamma_{\mathrm{D}}\right) < R_{th} \bigcap \mathcal{H}_0 \bigcap \gamma_{\mathrm{SD}} < \gamma_{th}\right] \sum_{i=\varphi}^{L} \xi_i + \Pr\left[\log_2\left(1+\gamma_{\mathrm{D}}\right) < R_{th} \bigcap \mathcal{H}_1 \bigcap \gamma_{\mathrm{SD}} < \gamma_{th}\right] \sum_{i=\varphi}^{L} \xi_i \\
&= \frac{1}{2} \sum_{i=\varphi}^{L} \xi_i \left\{ \underbrace{\Pr\left[\gamma_{\mathrm{D}} | \mathcal{H}_0 < 2^{R_{th}} - 1 \bigcap \gamma_{\mathrm{SD}} < \gamma_{th}\right]}_{f_1} + \underbrace{\Pr\left[\gamma_{\mathrm{D}} | \mathcal{H}_1 < 2^{R_{th}} - 1 \bigcap \gamma_{\mathrm{SD}} < \gamma_{th}\right]}_{f_2} \right\}
\end{aligned} \tag{58}
$$

f_2, which can be achieved by simply replacing variable x in (38) and (39) with factor $2^{R_{th}} - 1$. Substituting f_1 and f_2 into (58), we can derive the closed-form expression of the TOP in the FD SWIPT mode as (40).

Appendix H
Proof of Theorem 5

Similar to the derivation of (40), in the PEH mode, the TOP should be constructed as

$$
\begin{aligned}
TOP_{\mathrm{PEH}} &= \Pr\left[\log_2\left(1+\gamma_{\mathrm{D}}\right) < R_{th} \bigcap \mathrm{PEH}\right] \\
&= \underbrace{\Pr\left(\gamma_{\mathrm{SD}} < 2^{R_{th}} - 1 \cap \gamma_{\mathrm{SD}} < \gamma_{th}\right)}_{f_3} \sum_{i=0}^{\varphi-1} \xi_i \\
&\quad + \underbrace{\Pr\left(\gamma_{\mathrm{SD}} < 2^{R_{th}} - 1 \cap \gamma_{\mathrm{SD}} \geq \gamma_{th}\right)}_{f_4}.
\end{aligned} \tag{59}
$$

In the case of $\{\gamma_{\mathrm{SD}} < \gamma_{th}\} \cap \{E_i < E_{th}\}$, we have $\Pr\left(\gamma_{\mathrm{SD}} < 2^{R_{th}} - 1\right) = 1$. It is worth noting that hereby $\Pr\left(\gamma_{\mathrm{SD}} < 2^{R_{th}} - 1\right)$ and $\Pr\left(\gamma_{\mathrm{SD}} < \gamma_{th}\right)$ are independent with each other, because D ceases signal processing and forces $\Pr\left(\gamma_{\mathrm{SD}} < 2^{R_{th}} - 1\right) = 1$, leading to $f_3 = \Pr\left(\gamma_{\mathrm{SD}} < \gamma_{th}\right) = q_{\mathrm{SD}}$. In the case of $\gamma_{\mathrm{SD}} \geq \gamma_{th}$, the main wireless channel is good enough, the closed-form expression of CDF of $\gamma_{\mathrm{SD}} | \gamma_{\mathrm{SD}} \geq \gamma_{th}$ can be derived as

$$
\begin{aligned}
&F_{\gamma_{\mathrm{SD}} | \gamma_{\mathrm{SD}} \geq \gamma_{th}}\left(x\right) \\
&\quad = \begin{cases} \exp\left(-\dfrac{\sigma_{\mathrm{D}}^2 \gamma_{th}}{P_{\mathrm{S}} \Omega_{\mathrm{SD}}}\right) - \exp\left(-\dfrac{\sigma_{\mathrm{D}}^2 x}{P_{\mathrm{S}} \Omega_{\mathrm{SD}}}\right), & x > \gamma_{th} \\ 0, & x \leq \gamma_{th}. \end{cases}
\end{aligned} \tag{60}
$$

Hence, the closed-form expression of f_4 is given by $f_4 = F_{\gamma_{\mathrm{SD}} | \gamma_{\mathrm{SD}} \geq \gamma_{th}}\left(2^{R_{th}} - 1\right)$. Substituting f_3 and f_4 into (59), we derive the closed-form expression of the TOP in the PEH mode as (41).

References

[1] Z. Nie, R. Zhao, Y. Li, and X. Tan, "A full-duplex SWIPT relaying protocol based on discrete energy state," in *Proc. 20th Int. Symp. Wireless Pers. Multimedia Commun. (WPMC)*, Bali, Indonesia, Dec. 2017, pp. 500–505.

[2] L. R. Varshney, "Transporting information and energy simultaneously," in *Proc. IEEE Int. Symp. Inf. Theory*, Toronto, ON, Canada, Jul. 2008, pp. 1612–1616.

[3] R. Zhang and C. K. Ho, "MIMO broadcasting for simultaneous wireless information and power transfer," *IEEE Trans. Wireless Commun.*, vol. 12, no. 5, pp. 1989–2001, May 2013.

[4] I. Krikidis, "Simultaneous information and energy transfer in large-scale networks with/without relaying," *IEEE Trans. Commun.*, vol. 62, no. 3, pp. 900–912, Mar. 2014.

[5] X. Chen, D. W. K. Ng, W. H. Gerstacker, and H.-H. Chen, "A survey on multiple-antenna techniques for physical layer security," *IEEE Commun. Surveys Tuts.*, vol. 19, no. 2, pp. 1027–1053, 2nd Quart., 2017.

[6] G. Pan *et al.*, "On secrecy performance of MISO SWIPT systems with TAS and imperfect CSI," *IEEE Trans. Commun.*, vol. 64, no. 9, pp. 3831–3843, Sep. 2016.

[7] M. Zhang, K. Cumanan, L. Ni, H. Hu, A. G. Burr, and Z. Ding, "Robust beamforming for AN aided MISO SWIPT system with unknown eavesdroppers and non-linear EH model," in *Proc. IEEE Globecom Workshops (GC Wkshps)*, Abu Dhabi, United Arab Emirates, Dec. 2018, pp. 1–7.

[8] Z. Chu *et al.*, "Resource allocation for secure wireless powered integrated multicast and unicast services with full duplex self-energy recycling," *IEEE Trans. Wireless Commun.*, vol. 18, no. 1, pp. 620–636, Jan. 2019.

[9] D. Zhang, Y. Liu, L. Dai, A. K. Bashir, A. Nallanathan, and B. Shim, "Performance analysis of decentralized V2X system with FD-NOMA," in *Proc. IEEE 90th Veh. Technol. Conf. (VTC-Fall)*, Honolulu, HI, USA, Sep. 2019, pp. 1–6.

[10] D. Wang, R. Zhang, X. Cheng, L. Yang, and C. Chen, "Relay selection in full-duplex energy-harvesting two-way relay networks," *IEEE Trans. Green Commun. Netw.*, vol. 1, no. 2, pp. 182–191, Jun. 2017.

[11] H. Liu, K. J. Kim, K. S. Kwak, and H. Vincent Poor, "Power splitting-based SWIPT with decode-and-forward full-duplex relaying," *IEEE Trans. Wireless Commun.*, vol. 15, no. 11, pp. 7561–7577, Nov. 2016.

[12] K. Shahzad, X. Zhou, S. Yan, J. Hu, F. Shu, and J. Li, "Achieving covert wireless communications using a full-duplex receiver," *IEEE Trans. Wireless Commun.*, vol. 17, no. 12, pp. 8517–8530, Dec. 2018.

[13] S. Yan, Y. Cong, S. V. Hanly, and X. Zhou, "Gaussian signalling for covert communications," *IEEE Trans. Wireless Commun.*, vol. 18, no. 7, pp. 3542–3553, Jul. 2019.

[14] B. A. Bash, D. Goeckel, and D. Towsley, "Limits of reliable communication with low probability of detection on AWGN channels," *IEEE J. Sel. Areas Commun.*, vol. 31, no. 9, pp. 1921–1930, Sep. 2013.

[15] D. Goeckel, B. Bash, S. Guha, and D. Towsley, "Covert communications when the warden does not know the background noise power," *IEEE Commun. Lett.*, vol. 20, no. 2, pp. 236–239, Feb. 2016.

[16] J. Hu, S. Yan, F. Shu, and J. Wang, "Covert transmission with a self-sustained relay," *IEEE Trans. Wireless Commun.*, vol. 18, no. 8, pp. 4089–4102, Aug. 2019.

[17] J. Hu, S. Yan, X. Zhou, F. Shu, J. Li, and J. Wang, "Covert communication achieved by a greedy relay in wireless networks," *IEEE Trans. Wireless Commun.*, vol. 17, no. 7, pp. 4766–4779, Jul. 2018.

[18] J. Wang, W. Tang, Q. Zhu, X. Li, H. Rao, and S. Li, "Covert communication with the help of relay and channel uncertainty," *IEEE Wireless Commun. Lett.*, vol. 8, no. 1, pp. 317–320, Feb. 2019.

[19] Y. Bi and H. Chen, "Accumulate and jam: Towards secure communication via a wireless-powered full-duplex jammer," *IEEE J. Sel. Topics Signal Process.*, vol. 10, no. 8, pp. 1538–1550, Dec. 2016.

[20] G. Li and H. Jiang, "Performance analysis of wireless powered incremental relaying networks with an adaptive harvest-store-use strategy," *IEEE Access*, vol. 6, pp. 48531–48542, 2018.

[21] Z. Chu, K. Cumanan, Z. Ding, M. Johnston, and S. Y. Le Goff, "Secrecy rate optimizations for a MIMO secrecy channel with a cooperative jammer," *IEEE Trans. Veh. Technol.*, vol. 64, no. 5, pp. 1833–1847, May 2015.

[22] X. Zhou, S. Yan, J. Hu, J. Sun, J. Li, and F. Shu, "Joint optimization of a UAV's trajectory and transmit power for covert communications," *IEEE Trans. Signal Process.*, vol. 67, no. 16, pp. 4276–4290, Aug. 2019.

[23] R. Zhao, Y. Yuan, L. Fan, and Y.-C. He, "Secrecy performance analysis of cognitive decode-and-forward relay networks in Nakagami-m fading channels," *IEEE Trans. Commun.*, vol. 65, no. 2, pp. 549–563, Feb. 2017.
[24] Y. Li, R. Zhao, X. Tan, and Z. Nie, "Secrecy performance analysis of artificial noise aided precoding in full-duplex relay systems," in *Proc. GLOBECOM - IEEE Global Commun. Conf.*, Singapore, Dec. 2017, pp. 1–6.
[25] Z. Li, H. Chen, Y. Li, and B. Vucetic, "Incremental accumulate-then-forward relaying in wireless energy harvesting cooperative networks," in *Proc. IEEE Global Commun. Conf. (GLOBECOM)*, Washington, DC, USA, Dec. 2016, pp. 1–6.
[26] T. V. Sobers, B. A. Bash, S. Guha, D. Towsley, and D. Goeckel, "Covert communication in the presence of an uninformed jammer," *IEEE Trans. Wireless Commun.*, vol. 16, no. 9, pp. 6193–6206, Sep. 2017.
[27] M. Shaked and J. G. Shanthikumar, *Stochastic Orders and Their Applications*. New York, NY, USA: Academic, 1994.

Yuanjian Li received the B.Eng. degree in information and communication engineering from the Faculty of Computer Science and Technology, Nanjing Tech University, Nanjing, China, in 2015, and the M.Eng. degree in information and communication engineering from the Faculty of Information Science and Engineering, Huaqiao University, Xiamen, China, in 2019. He is currently pursuing the Ph.D. degree with the Department of Engineering, Faculty of Natural and Mathematical Sciences, King's College London, London, U.K. His current research interests include UAV-aided wireless networks, machine learning, and radio resource management.

Rui Zhao (Member, IEEE) received the dual bachelor's degree from the Harbin Institute of Technology and the M.S. and Ph.D. degrees in electrical engineering from Southeast University, China, in 2003, 2006, and 2010, respectively. After graduation, he joined the School of Information Science and Engineering, Huaqiao University, China, where he is currently an Associate Professor. From March 2014 to March 2015, he visited the Department of Electronic and Computer Engineering, Hong Kong University of Science and Technology (HKUST), Hong Kong, where he was a Visiting Research Scholar. His current research interests include wireless communications, physical-layer security, and machine learning. He has published many articles in international journals, such as the IEEE TRANSACTIONS ON WIRELESS COMMUNICATIONS and the IEEE TRANSACTIONS ON COMMUNICATIONS.

Yansha Deng (Member, IEEE) received the Ph.D. degree in electrical engineering from the Queen Mary University of London, U.K., in 2015. From 2015 to 2017, she was a Post-Doctoral Research Fellow with King's College London, U.K., where she is currently a Lecturer (an Assistant Professor) with the Department of Engineering. Her research interests include molecular communication and machine learning for 5G/B5G wireless networks. She was a recipient of the best paper awards from ICC 2016 and Globecom 2017 as the first author. She is also an Associate Editor of the IEEE TRANSACTIONS ON COMMUNICATIONS, the IEEE TRANSACTIONS ON MOLECULAR, BIOLOGICAL AND MULTI-SCALE COMMUNICATIONS, and the Senior Editor of the IEEE COMMUNICATIONS LETTERS. She also received the Exemplary Reviewers of the IEEE TRANSACTIONS ON COMMUNICATIONS in 2016 and 2017, and the IEEE TRANSACTIONS ON WIRELESS COMMUNICATIONS in 2018. She has also served as a TPC Member for many IEEE conferences, such as the IEEE GLOBECOM and ICC.

Feng Shu (Member, IEEE) was born in 1973. He received the B.S. degree from Fuyang Teaching University, Fuyang, China, in 1994, the M.S. degree from Xidian University, Xi'an, China, in 1997, and the Ph.D. degree from Southeast University, Nanjing, China, in 2002. Since 2005, he has been working with the School of Electronic and Optical Engineering, Nanjing University of Science and Technology, Nanjing. From 2009 to 2010, he held a visiting Post-Doctoral Researcher position with The University of Texas at Dallas. Since 2020, he has also been with the School of Information and Communication Engineering, Hainan University, Haikou, China, where he is currently a Professor, and also a Supervisor of the Ph.D. and graduate students. He has published about 300 articles, of which more than 200 are in archival journals, including more than 100 articles in the IEEE JOURNALS and more than 130 SCI-indexed articles. He holds 13 Chinese patents. His research interests include wireless networks, wireless location, and array signal processing. He serves as a TPC Member for several international conferences, including the IEEE ICC 2019, the IEEE VTC2020, ICCS 2018/2016, ISAPE 2018, and WCSP 2017/2016/2014. He was a Mingjiang Chair Professor and hundreds-of-talented plan in Fujian Province. He is also an Associate Editor of the IEEE SYSTEMS JOURNAL and the IEEE ACCESS JOURNAL.

Zhiqiao Nie received the B.Eng. and M.Eng. degree in information and communication engineering from the College of Information Engineering and Technology, Xiamen University of Technology, Xiamen, China, in 2015, and the M.Eng. degree in information and communication engineering from the Faculty of Information Science and Engineering, Huaqiao University, Xiamen, China, in 2018. He is currently an Engineer working with Xiamen Meiya Pico Information Company, Ltd. His current research interests include machine learning and image processing.

A. Hamid Aghvami (Life Fellow, IEEE) joined the academic staff at King's College London in 1984. In 1989, he was promoted to a Reader, and in 1993 was promoted to a Professor in telecommunications engineering. He is currently the Founder of the Centre for Telecommunications Research at King's. He was the Director of the Centre from 1994 to 2014. He carries out consulting work on Digital Radio Communications Systems for British and International companies. He has published more than 560 technical journals and conference papers, filed 30 patents and given invited talks and courses the world over on various aspects of Mobile Radio Communications. He was a Visiting Professor with NTT Radio Communication Systems Laboratories in 1990, a Senior Research Fellow with BT Laboratories from 1998 to 1999, and was an Executive Advisor to Wireless Facilities Inc., USA, from 1996 to 2002. He is the Chairman of the Advanced Wireless Technology Group Ltd. He is also the Managing Director of Wireless Multimedia Communications Ltd., his own consultancy company. He is also a Visiting Professor with Imperial College. He also leads an active Research Team working on numerous mobile and personal communications projects for Fourth and Fifth generation networks; these projects are supported by both government and industry. He was a member of the Board of Governors of the IEEE Communications Society from 2001 to 2003, and was a Distinguished Lecturer of the IEEE Communications Society from 2004 to 2007. He has been a member, the Chairman, and the Vice-Chairman of the technical programme and organizing committees of a large number of international conferences. He is also Founder of the International Symposium on Personal Indoor and Mobile Radio Communications (PIMRC), a major yearly conference attracting around 1,000 attendees. He was awarded the IEEE Technical Committee on Personal Communications (TCPC) Recognition Award in 2005 for his outstanding technical contributions to the communications field, and for his service to the scientific and engineering communities. He is a fellow of the Royal Academy of Engineering, fellow of the IET, and in 2009 was awarded a Fellowship of the Wireless World Research Forum in recognition of his personal contributions to the wireless world, and for his research achievements as the Director of the Centre for Telecommunications Research at King's.